Journal of Ethnopharmacology 362 (2026) 121267

Contents lists available at ScienceDirect

Journal of Ethnopharmacology

journal homepage: www.elsevier.com/locate/jethpharm

Comprehensive evaluation of the anti-inflammatory potential of *Cucurbita maxima* leaf extract: LC–MS phytochemical profiling coupled with *in vitro*, *in vivo*, and *in silico* approaches

Hammadi Maroua [a], Mohammed Larbi Benamor [a], Yahia Bekkar [a], Salah Neghmouche Nacer [b], Elhafnaoui Lanez [a], Ouafa Boudebia [a], Housseyn Chaoua [a], Aicha Adaika [a], Lazhar Bechki [c], Touhami Lanez [a], Stefania Garzoli [d,*]

[a] University of El Oued, Faculty of Exact Sciences, Department of Chemistry, VTRS Laboratory, B.P.789, 39000, El Oued, Algeria
[b] Department of Chemistry, Faculty of Exact Sciences, University of El Oued, P.O. Box 789, El Oued, 39000, Algeria
[c] Kasdi Merbah University, VPRS Laboratory, Department of Chemistry, Faculty of Mathematics and Material Sciences, 30000, Ouargla, Algeria
[d] Department of Chemistry and Technologies of Drug, Sapienza University, P. le Aldo Moro, 5, 00185, Rome, Italy

ARTICLE INFO

Keywords:
Cucurbita maxima leaves
Anti-inflammatory activity
Polyphenols
UPLC–ESI–MS/MS
Molecular docking
Cyclooxygenase-1 (COX-1)
ADMET prediction

ABSTRACT

Ethnopharmacological relevance: *Cucurbita maxima* (pumpkin) leaves have been traditionally used in folk medicine for the treatment of inflammation, fever, and oxidative stress–related disorders. However, scientific validation of these claims remains limited. This study aimed to evaluate the anti-inflammatory, antioxidant, and protective effects of *C. maxima* leaf aqueous extract and to elucidate its phytochemical composition and molecular mechanisms of action.

Materials and methods: The phytochemical profile of the aqueous extract was determined using UPLC–ESI–MS/MS analysis. In vivo anti-inflammatory activity was assessed in a benzylthiouracil-induced inflammation model by measuring white blood cell (WBC) counts, C-reactive protein (CRP) levels, and histopathological changes in liver and kidney tissues. In vitro anti-inflammatory potential was evaluated through the protein denaturation inhibition assay, using diclofenac as a reference. Pharmacokinetic and toxicity properties of major compounds were predicted using ADMET tools, while molecular docking studies were performed to evaluate interactions with COX-1 and COX-2 enzymes.

Results: UPLC–ESI–MS/MS analysis revealed a complex mixture of polyphenols, with caffeic acid (56.04%), rutin (9.25%), ferulic acid (8.79%), and myricetin-3-rhamnose (8.62%) as the main constituents. The extract significantly reduced inflammation by normalizing WBC counts (from 7.2 to 4.5 $\times$ 10^9/L), lowering CRP levels (from 630 to 220 mg/L), and protecting liver and kidney tissues. The extract also inhibited protein denaturation in vitro (IC_{50} = 2.976 mg/mL) compared to diclofenac (IC_{50} = 0.718 mg/mL). Molecular docking revealed that major flavonoids exhibited strong binding affinities toward COX-1 and COX-2, often surpassing diclofenac, supported by stable hydrogen bonding and hydrophobic interactions. ADMET and toxicity predictions indicated good intestinal absorption for several major compounds, absence of predicted hepatotoxicity or skin sensitization, and generally low acute toxicity, with high predicted LD_{50} values and no mutagenic risk for most constituents.

Conclusion: These findings support the traditional use of *C. maxima* leaves in folk medicine for the management of inflammation-related conditions, fever, and associated oxidative stress. Further isolation of the key active constituents and clinical evaluation are recommended to confirm their therapeutic efficacy.

* Corresponding author.
E-mail addresses: hammadi-maroua@univ-eloued.dz (H. Maroua), benamor-mohmmedlarbi@univ-eloued.dz (M. Larbi Benamor), neghmouchenacer-salah@univ-eloued.dz (S. Neghmouche Nacer), lanez-elhafnaoui@univ-eloued.dz (E. Lanez), boudebia-ouafa@univ-eloued.dz (O. Boudebia), housseyn-chaoua@univ-eloued.dz (H. Chaoua), adaikaicha@gmail.com (A. Adaika), lbechki1@gmail.com (L. Bechki), touhami-lanez@univ-eloued.dz (T. Lanez), stefania.garzoli@uniroma1.it (S. Garzoli).

https://doi.org/10.1016/j.jep.2026.121267
Received 13 November 2025; Received in revised form 13 January 2026; Accepted 26 January 2026
Available online 2 February 2026

Abbreviation	Meaning
ADMET	Absorption, Distribution, Metabolism, Excretion, Toxicity
ALT	Alanine aminotransferase
ANOVA	Analysis of variance
AST	Aspartate aminotransferase
BSA	Bovine Serum Albumin
BTU	Benzylthiouracil
COX-1	Cyclooxygenase-1
COX-2	Cyclooxygenase-2
CRP	C-reactive protein
CT	Creatinine
DMSO	Dimethyl sulfoxide
EDTA	Ethylenediaminetetraacetic acid
FBS	Fasting Blood Sugar
H&E	Hematoxylin and Eosin
HGB	Hemoglobin
IC_{50}	Half maximal inhibitory concentration
IBU	Ibuprofen
IL-1β	Interleukin-1 beta
LC–MS/MS	Liquid Chromatography Tandem Mass Spectrometry
LGA	Lamarckian Genetic Algorithm
LYM	Lymphocytes
MAPKs	Mitogen-activated protein kinases
NF-κB	Nuclear factor-kappa B
NO	Nitric oxide
PDB	Protein Data Bank
PK	Pharmacokinetics
PL	Pumpkin Leaves extract
RBC	Red Blood Cells
ROS	Reactive Oxygen Species
SD	Standard Deviation
SDF	Structure-Data File
TNF-α	Tumor Necrosis Factor alpha
UHPLC	Ultra-High Performance Liquid Chromatography
UV–Vis	Ultraviolet–Visible spectroscopy
WBC	White Blood Cells

1. Introduction

Inflammation is a vital defense mechanism of the body, activated in response to infections, toxins, and tissue damage. It plays a central role in eliminating harmful agents and initiating repair processes. However, when the inflammatory response becomes prolonged or uncontrolled, it can contribute to the onset and progression of chronic disorders such as arthritis, cardiovascular diseases, metabolic syndrome, neurodegenerative conditions, and certain cancers (Nathan and Ding, 2010; Libby, 2007). This process involves the recruitment and activation of immune cells, leading to the release of pro-inflammatory mediators such as cytokines, prostaglandins, nitric oxide, and reactive oxygen species. (Kany et al., 2019). These mediators activate transcription factors like nuclear factor-kappa B (NF-κB) and mitogen-activated protein kinases (MAPKs), amplifying inflammatory signaling (Lawrence, 2009). Persistent activation of such pathways can damage tissues and maintain a chronic inflammatory state. These limitations have driven increasing interest in medicinal plants as safer alternatives, owing to their multi-target anti-inflammatory actions and favorable antioxidant profiles.

Current anti-inflammatory therapies, including nonsteroidal anti-inflammatory drugs (NSAIDs) and corticosteroids, are effective in symptom control but are often limited by serious side effects during long-term use, such as gastrointestinal lesions, liver and kidney toxicity, and elevated cardiovascular risk (Farkouh et al., 2022). It lead to a growing interest in medicinal plants as safer sources of anti-inflammatory compounds with multitargeted actions and antioxidant potential (Calixto, 2019).

Among promising medicinal plants, *Cucurbita maxima* Duchesne (commonly known as winter squash or pumpkin), belonging to the Cucurbitaceae family, has been traditionally used in the treatment of wounds, swelling, and chronic ailments (Salehi et al., 2019). Phytochemical studies reveal that this species contains a rich diversity of secondary metabolites, including flavonoids, phenolic acids, carotenoids, terpenoids, cucurbitacins, and unsaturated fatty acids (Altaf et al., 2025). These bioactive constituents contribute to reducing oxidative stress, an important driver of chronic inflammation, by scavenging free radicals and enhancing endogenous antioxidant defenses. Previous pharmacological reports highlight significant anti-inflammatory and antioxidant activities of *Cucurbita maxima* extracts, particularly from seeds and fruits. (Rahman and McFadden, 2011).

Experimental findings suggest that the plant's extracts can inhibit NF-κB activation, suppress the expression of cyclooxygenase-2 (COX-2) and inducible nitric oxide synthase (iNOS), and reduce the production of prostaglandins and NO(Weremczuk-Jeżyna et al., 2023). Phenolic compounds such as gallic acid, ellagic acid, luteolin, and apigenin are known to modulate cytokine production and limit oxidative tissue injury (Leyva-López et al., 2016). In vivo models have demonstrated reduced leukocyte infiltration, restoration of antioxidant enzyme levels, and attenuation of tissue damage following administration of *C. maxima* extracts (Neamah et al., 2023). Computational studies further indicate strong interactions between its phytochemicals and COX enzymes, supporting their potential as anti-inflammatory agents. These compounds also exhibit favorable pharmacokinetic and safety profiles, reinforcing their therapeutic promise (Alqahtani, 2017; Morris et al., 2009).

C. maxima also carries cultural and historical significance. In the Qur'anic account of the Prophet Yunus (peace be upon him), following his deliverance from the whale, God caused a gourd plant to grow above him, providing food, shade, and healing: "And caused a squash plant to grow over him" [As-Saffat: 146]. This reference underlines the long-standing recognition of gourds in health and healing traditions.

In light of both ethnomedicinal knowledge and emerging scientific data, this study investigates the anti-inflammatory potential of aqueous extracts from *C. maxima* leaves through a multidisciplinary approach. Using LC–MS/MS metabolite profiling, in vitro protein denaturation assays, an in vivo benzylthiouracil-induced inflammation model, and in silico molecular docking, we aim to identify active constituents, evaluate biological efficacy, and clarify possible mechanisms of action. This work provides comprehensive evidence to support the development of *C. maxima* leaves as a safe and effective source of anti-inflammatory agents.

Although various parts of *Cucurbita maxima*, particularly seeds and fruits, have been extensively investigated for their nutritional and pharmacological properties, studies focusing on the leaves remain scarce. To the best of our knowledge, no previous work has reported a comprehensive evaluation of the anti-inflammatory potential of *C. maxima* leaf aqueous extract integrating phytochemical profiling by LC–MS/MS with in vitro, in vivo, and in silico approaches. The present study addresses this gap by specifically investigating the leaves, an underexplored plant part, and by combining experimental and computational methods to provide mechanistic insight into their anti-inflammatory and organ-protective effects.

2. Materials and methods

2.1. Plant material

Fresh, fully developed leaves of *Cucurbita maxima* Duchesne (Cucurbitaceae) were harvested between October and November 2024 from the Trifaoui locality in El Oued Province, southeastern Algeria (20°33′ N, 53°6′ E). The site lies roughly 600 km inland from the Mediterranean coast at an elevation of about 80 m above sea level. The region experiences an arid desert climate, characterized by minimal annual rainfall and marked day–night temperature fluctuations. Botanical identification was carried out by an experienced taxonomist, and a reference voucher (specimen code: VBRS-2024-9) was deposited in the VTRS herbarium.

2.2. Preparation of plant extracts

Aqueous maceration was selected to preserve thermolabile, water-soluble constituents (Manimaran et al., 2025; Suhendra et al., 2025). Dried leaf powder (100 g) was mixed with distilled water (1000 mL; 1:10, w/v) in sealed glass containers and kept in the dark at room temperature for 24 h with intermittent stirring. The procedure was repeated three times with fresh solvent to maximize recovery (Duistermaat and Kolk, 2000). Each batch was filtered through Whatman No. 2 paper; the filtrates were pooled and concentrated under reduced pressure at 45 °C and 5 ± 2 mbar using a Büchi Rotavapor R-200 with a B-490 heating bath and V-3300 pump (Joshi et al., 2025). The concentrate was freeze-dried (SED-XDG laboratory freeze dryer) to protect thermolabile constituents and obtain a stable dry powder, using freezing followed by low-pressure sublimation to preserve bioactivity (Ertas and Yener, 2020; Madi et al., 2025).

The extraction process yielded 12.4% (w/w) of dry extract relative to the initial dried leaf material.

2.3. Ultra-performance liquid chromatography–tandem mass spectrometry analysis

Analyses were carried out on a Nexera UHPLC (Shimadzu, USA) coupled to a triple-quadrupole mass spectrometer (LCMS-8040, Shimadzu) (Lekmine et al., 2020). Separation employed an Inertsil ODS-4 C18 column (150 mm × 4.6 mm, 3 µm) at 40 °C. Mobile phase A was water with ammonium formate (5 mM) and formic acid (0.1%), and mobile phase B was methanol with ammonium formate (5 mM) and formic acid (0.1%). A gradient was delivered at 0.5 mL/min with a 4 µL injection. Electrospray ionization (ESI) conditions were: desolvation line 250 °C, interface 350 °C, heat block 400 °C, drying gas 15 L/min, nebulizing gas 3 L/min.

Analytical characteristics (linearity ranges and regression statistics) followed previously reported LC–MS/MS validations (Ertas and Yener, 2020; Madi et al., 2025). Calibration curves were linear and reproducible ($R^2 > 0.991$). Reported LOD and LOQ values were 0.05–25.8 µg/L and 0.17–85.9 µg/L, respectively, with recoveries for phenolic compounds of 96.9–106.2% (Jumepaeng and Pongpun, 2020; Kara et al., 2022).

2.4. In vivo evaluation of anti-inflammatory activity

2.4.1. Animal care

Twenty adults male Wistar rats (150–200 g) were obtained from the Pasteur Institute (Algiers). Animals were acclimatized for 15 days under controlled conditions (25 ± 2 °C; 62% humidity; 12 h light/dark) with ad libitum access to standard chow formulated according to established guidance (Kunchandy and Rao, 1990) and tap water. All procedures were approved by the Scientific Council Committee of the Faculty of Natural Sciences and Life, University of El Oued, and complied with institutional ethical standards (Elhewehy et al., 2025). All procedures were approved by the Scientific Council Committee of the Faculty of Natural Sciences and Life, University of El Oued (El Oued, Algeria), under ethical approval reference number: 29/S.C/F.L.N.S/E.U/2025, and were conducted in accordance with internationally accepted guidelines for the care and use of laboratory animals.

2.4.2. Induction of internal organ inflammation

Benzylthiouracil (BTU) was administered by oral gavage at 2 mg/kg body weight (1 mL per rat) once daily for 21 days to induce internal organ inflammation. Although benzylthiouracil (BTU) is primarily used as an antithyroid agent, chronic BTU administration has been reported to induce systemic inflammatory alterations secondary to thyroid dysfunction, oxidative stress, and immune imbalance. Experimental studies have shown that prolonged BTU exposure leads to leukocytosis, elevated C-reactive protein levels, increased pro-inflammatory cytokine release, and concomitant hepatic and renal injury, thereby establishing a sustained inflammatory state. These pathophysiological changes make the BTU model suitable for investigating anti-inflammatory and organ-protective effects of bioactive compounds, particularly in the context of inflammation-associated metabolic and endocrine disturbances.

2.4.3. Experimental design

Following confirmation of inflammation, rats were randomized into groups (n = 5).

- Group I (Control): standard diet and water only.
- Group II (BTU): BTU 2 mg/kg/day by oral gavage (Diemar et al., 2025).
- Group III (BTU + PL): BTU for 21 days, then *C. maxima* leaf extract 100 mg/kg/day, p.o.
- Group IV (BTU + IBU): BTU for 21 days, then ibuprofen 2 mg/kg/day, p.o.

Post-induction treatments were continued for 21 days.

The sample size (n = 5 animals per group) was selected in accordance with commonly accepted practices in exploratory in vivo pharmacological studies and is consistent with previous reports using similar inflammatory and organ injury models, ensuring adequate statistical power while adhering to ethical principles aimed at minimizing animal use.

2.4.4. Blood and organ collection

After 16 h of fasting, animals were anesthetized using an intraperitoneal injection of ketamine (80 mg/kg) and xylazine (10 mg/kg), followed by humane sacrifice. Blood samples were collected immediately post-mortem; one portion was placed into EDTA-containing tubes for hematological analysis, while the other portion was collected in plain tubes for serum-based biochemical testing. Subsequently, vital organs and tissues-including the kidneys, and liver were carefully excised. Each tissue was rinsed thoroughly with distilled water followed by physiological saline (0.9% NaCl), gently dried with sterile filter paper, weighed with precision and fixed in 10% neutral buffered formalin for 24 h at room temperature prior to paraffin embedding and histological processing.

2.4.5. In vitro evaluation of anti-inflammatory activity

2.4.5.1. Bovine serum albumin (BSA) denaturation assay. The anti-denaturation assay followed established methodology with minor modifications (M et al., 2023). Reaction mixtures contained 500 µL of 5% BSA and 250 µL of test sample (100–1000 µg/mL). Diclofenac sodium served as the positive control; the negative control comprised BSA mixed with distilled water. Mixtures were incubated at 37 °C for 20 min, heated at 70 °C for 20 min, cooled to room temperature, diluted with 500 µL deionized water, and read at 660 nm (UV–Vis). A blank contained 1 mL water +250 µL DMSO. Percent inhibition was calculated as:

$$\%\ \text{Inhibition} = \left(\frac{A_{control} - A_{sample}}{A_{control}}\right) \times 100$$

Where $A_{control}$ corresponds to the absorbance of the negative control, and A_{sample} represents the absorbance of the test sample or positive control. All experiments were performed in triplicate, and the results were expressed as mean ± standard deviation (SD).

2.5. In silico evaluation of anti-inflammatory activity

2.5.1. ADMET and drug-likeness prediction

The pharmacokinetic behavior and drug-likeness of the bioactive compounds from the aqueous leaf extract of *Cucurbita maxima* were evaluated through ADMET (Absorption, Distribution, Metabolism,

Excretion, and Toxicity) profiling using the SwissADME and pkCSM platforms (Daina et al., 2017; Pires et al., 2015). The analysis aimed to identify molecules with favorable oral bioavailability and pharmacokinetic properties relevant to anti-inflammatory therapy.

2.5.2. Docking setup

The three-dimensional (3D) structures of the major bioactive compounds from *Cucurbita maxima* leaves were obtained from the PubChem database in SDF format and converted to PDB format using Open Babel (Kim et al., 2023; O'Boyle et al., 2011). Ligand geometries were optimized through energy minimization with the MMFF94 force field to generate stable conformations suitable for docking.

Molecular docking was carried out in AutoDock Tools (version 1.5.7) (Eberhardt et al., 2021) using the Lamarckian Genetic Algorithm (LGA) to predict the most favorable binding conformations between the ligands and the selected protein targets (Adaika et al., 2025; Larbi et al., 2025). Before docking, ligands and proteins were converted into PDBQT format, with Gasteiger charges assigned and torsional degrees of freedom defined. For each protein, the grid box was configured to fully encompass the active site, ensuring comprehensive sampling of potential binding regions.

The crystal structures of bovine serum albumin (BSA; PDB ID: 6QS9), cyclooxygenase-1 (COX-1; PDB ID: 1EQG), and cyclooxygenase-2 (COX-2; PDB ID: 1PXX) were retrieved from the RCSB Protein Data Bank (Berman et al., 2000). All protein structures were prepared following standard protocols (Bekkar et al., 2025; T. Lanez et al., 2025), which involved the removal of crystallographic water molecules and nonessential heteroatoms, followed by conversion into AutoDock-compatible PDBQT format for molecular docking analysis. Docking results were examined using LigPlot v2.3 (Laskowski and Swindells, 2011).

2.6. Statistical analysis

In the present study, all experimental data are expressed as mean ± standard deviation (SD) based on triplicate measurements. For datasets, one-way analysis of variance (ANOVA) was conducted to identify significant differences among groups, followed by Tukey's post hoc test for pairwise comparisons. Statistical significance was established at p-values less than 0.05. All statistical analyses were performed using GraphPad Prism (version 10), OriginPro 9.0 or SPSS (version 20), ensuring rigorous evaluation of the experimental results.

The definitions of all statistical symbols and significance thresholds are consistently reported in the corresponding table footnotes and figure captions to ensure clear interpretation of the results.

3. Results and discussion

3.1. LC-MS/MS profiling of Cucurbita maxima leaf aqueous extract

The aqueous extract of *Cucurbita maxima* leaves exhibited a diverse phytochemical composition, predominantly enriched in polyphenolic compounds with known anti-inflammatory activity. The major compounds identified by UPLC–ESI–MS/MS (Fig. 1) are summarized in Table 1.

The profile was clearly dominated by caffeic acid (56.04%), highlighting its central role as the most abundant compound. Other prominent constituents included rutin (9.25%), ferulic acid (8.79%), and myricetin-3-rhamnose (8.62%), which collectively contribute to the strong polyphenolic signature of the extract. These compounds are well-documented inhibitors of pro-inflammatory enzymes, particularly cyclooxygenase-2 (COX-2), and modulators of signaling pathways associated with inflammation and oxidative stress (Amrouche et al., 2020; Dhorajiwala et al., 2019).

Additionally, moderately abundant compounds such as hispidulin

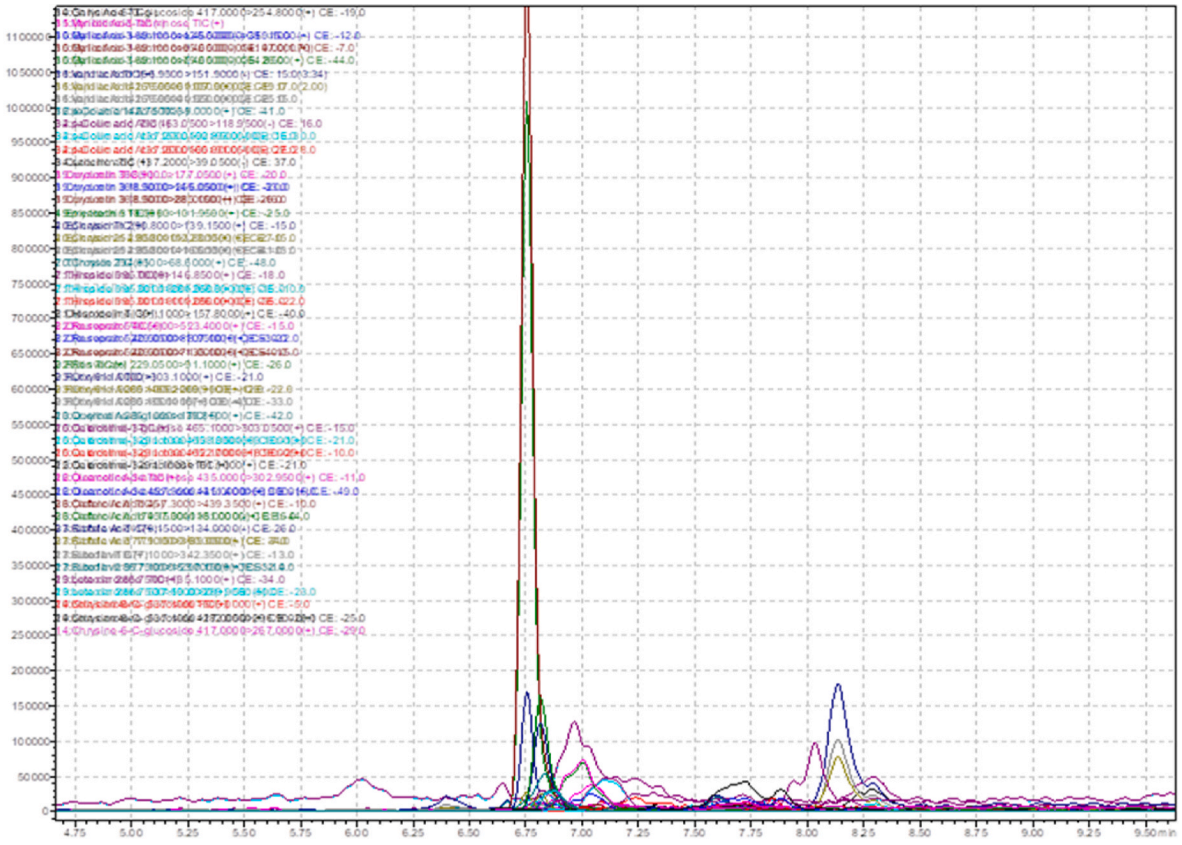

Fig. 1. LC-MS chromatogram of the *Cucurbita M* leaves extracts.

Table 1
Principal phytochemicals identified in *Cucurbita maxima* leaf aqueous extract.

N°	Compound Name	Relative Area (%)	Retention Time (min)	N°	Compound Name	Relative Area (%)	Retention Time (min)
1	Catechin (−)	3.67	8.033	18	Oleanolic Acid	0.00	0.000
2	Chrysin-6-C-glucoside	1.01	7.847	19	Oleuropein	0.98	7.730
3	Myricetin 3-arabinoside	0.00	0.000	20	Quercetin	0.11	6.827
4	Myricetin	2.49	7.037	21	Resveratrol	0.30	6.874
5	Myricetin-3-rhamnose	8.62	7.002	22	Riboflavin	7.29	8.136
6	Oxyline A	0.00	0.000	23	Rutin	9.25	6.814
7	Quercetin-3-arabinose	0.00	0.000	24	Sinapic Acid	8.60	6.907
8	Quercetin-3-glucoside	3.04	6.826	25	Beta Carotene	0.88	8.300
9	Tiliroside	0.13	6.873	26	Kojic Acid	0.97	6.398
10	Apigenin	0.09	7.063	27	Naringenin	0.00	0.000
11	Hispidulin	7.88	6.965	28	Thymol	0.65	7.207
12	2-Methoxybenzoic Acid	0.00	0.000	29	Vanillin	0.45	6.871
13	Chrysin	0.53	6.619	30	Caffeic Acid	56.04	6.754
14	Curcumin	0.22	6.637	31	Gallic Acid	0.02	1.191
15	Epicatechin	0.05	7.018	32	Vanillic Acid	0.06	1.157
16	Ferulic Acid	8.79	7.052	33	p-Coumaric Acid	1.47	6.903
17	Luteolin	0.00	0.000	34	Salicylic Acid	2.07	7.098

(7.88%) and riboflavin (7.29%) likely enhance the antioxidant potential, supporting the attenuation of inflammatory mediators. Other flavonoids, including quercetin-3-glucoside (3.04%), myricetin (2.49%), salicylic acid (2.07%), and catechin (3.67%), though present in lower amounts, may act synergistically to reinforce both anti-inflammatory and antioxidant effects.

Overall, the phytochemical composition presented in Table 1 provides a comprehensive picture of the bioactive constituents responsible for the pharmacological potential of *C. maxima* leaf extract, particularly its strong antioxidant and anti-inflammatory activities.

3.2. *In vivo anti-inflammatory activities*

3.2.1. *Hematological parameters*

The outcomes showed that the BTU administration induced significant leukocytosis illustrated in Table 2, with marked increases in WBC count from $4.1 \pm 0.2 \times 10^9$/L in the control group to $7.2 \pm 0.13 \times 10^9$/L ($p < 0.001$), also lymphocytes (LYM) rose from $3.7 \pm 0.62 \times 10^9$/L in the control to $5.5 \pm 0.21 \times 10^9$/L ($p < 0.001$), while granulocytes (GRA) increased from $0.2 \pm 0.04 \times 10^9$/L to $0.8 \pm 0.08 \times 10^9$/L ($p < 0.001$). while erythrocyte and thrombocyte indices (HGB, RBC, PLT) showed no significant differences compared with control values remained unaffected. The absence of significant differences between the BTU + PL group and the control group indicates a normalization of hematological parameters following treatment, reflecting a protective and inflammation-attenuating effect rather than a supraphysiological response. (Donate-Correa et al., 2020; Ng et al., 2025). Comparable findings have been reported in rodent models of chemically induced inflammation, where leukocyte elevation occurs without impairing erythropoiesis (Araújo et al., 2020).Co-treatment with pumpkin leaf extract (BTU + PL) are normalized WBC ($4.5 \pm 0.15 \times 10^9$/L) and GRA ($0.3 \pm 0.05 \times 10^9$/L) to near-control levels (NS*), and significantly reduced LYM counts to $4.6 \pm 0.3 \times 10^9$/L ($p < 0.01$, b), showing a more complete restoration than ibuprofen in our model and demonstrating a protective effect against BTU-induced leukocytosis. These results align with reports on other *Cucurbita* species demonstrated protective effects against inflammation and immune overactivation in rats (Mukherjee et al., 2022). Other studies have been shown to regulate immune functions such as phagocytosis and cytokine production.

Similarly, ibuprofen (BTU + IBU) attenuated these changes, lowering WBC to $5.67 \pm 0.43 \times 10^9$/L ($p < 0.05$, a), LYM to $4.3 \pm 0.05 \times 10^9$/L ($p < 0.05$), and GRA to $0.5 \pm 0.01 \times 10^9$/L ($p < 0.001$), confirming its strong anti-inflammatory action. The phytochemical profile of our extract dominated by caffeic acid, rutin, ferulic acid, and myricetin derivatives provides mechanistic support exerts leukocyte-normalizing effects comparable to ibuprofen but through broader polyphenol-driven pathways (Ha and Kim, 2006). Rutin has been shown to inhibit COX-2 expression and leukocyte recruitment (Nafees et al., 2015) [2], while ferulic acid attenuates leukocyte infiltration and inflammatory mediator release (Kaur et al., 2022; Srinivasan et al., 2007).

3.2.2. *Biochemical parameters*

BTU administration significantly disrupted hepatic and renal functions, as reflected by elevated AST, ALT, urea, and creatinine, while aspartate aminotransferase (AST) increased from 103.3 ± 4.48 U/L in the control to 189.15 ± 8.84 U/L ($p < 0.001$), alanine aminotransferase (ALT) rose from 32.95 ± 5.12 U/L to 42.13 ± 1.3 U/L ($p < 0.01$), indicating hepatocellular damage. Likewise, urea levels increased from 0.39 ± 0.17 g/L to 0.61 ± 0.11 g/L ($p < 0.001$), and creatinine (CT) rose from 3.81 ± 0.06 mg/L to 4.29 ± 0.03 mg/L ($p < 0.05$), reflecting impaired renal clearance (Table 3). In contrast, fasting blood sugar (FBS) remained unchanged (0.41 ± 0.21 g/L vs. 0.43 ± 0.24 g/L, NS). These alterations confirm BTU-induced hepato- and nephrotoxicity, which are often mediated by oxidative stress, lipid peroxidation, and inflammatory cytokine release (Arjumand et al., 2011; Pabla and Dong, 2008). The elevation of transaminases reflects hepatocellular membrane leakage, while the rise in urea and creatinine indicates impaired renal clearance and glomerular filtration (Li et al., 2023). Co-treatment with pumpkin leaf extract (BTU + PL) significantly restored AST (100.46 ± 2.3 U/L) and ALT (33.89 ± 1.35 U/L) to near-control levels (NS**), while partially improving urea (0.46 ± 0.12 g/L, $p < 0.05$ vs. BTU) and creatinine (3.26 ± 0.61 mg/L, NS). These effects indicate

Table 2
Plasma concentration of hematological parameters of different experimental groups.

	WBC($\times 10^9$/L)	LYM($\times 10^9$/L)	GRA ($\times 10^9$/L)	HGB (g/dL)	RBC($\times 10^{12}$/L)	PLT ($\times 10^9$/L)
Control	4.1 ± 0.2	3.7 ± 0.62	0.2 ± 0.04	14.46 ± 0.7	7.8 ± 0.47	969 ± 9.23
BTU	7.2 ± 0.13 ^{c}	5.5 ± 0.21^{a}	0.8 ± 0.08 ^{c}	14.4 ± 0.21^{NS}	7.9 ± 0.12 ^{NS}	976 ± 11.5 ^{NS}
BTU + PL	4.5 ± 0.15 ^{NS*}	4.6 ± 0.3 ^{b*}	0.3 ± 0.05 ^{NS*}	14.21 ± 0.7^{NS}	7.77 ± 0.51 ^{NS}	945.67 ± 5.4 ^{NS}
BTU + IBU	5.67 ± 0.43 ^{a*}	4.3 ± 0.05 ^{a*}	0.5 ± 0.01 ^{c}	14.6 ± 0.2 ^{NS}	7.3 ± 0.19 ^{NS}	961.3 ± 3.8 ^{NS}

Data are expressed as mean ± SD (n = 5). Statistical analysis was performed using one-way ANOVA followed by Tukey's post hoc test. *$p < 0.05$ (), $p < 0.01$ (), and $p < 0.001$ ()* indicate significant differences compared with the BTU group, while NS denotes non-significant differences.

Table 3
Glycemia, liver and kidney's function parameters of different experimental groups.

	FBS (g/L)	AST (U/L)	ALT (U/L)	Urea (g/L)	CT (mg/L)
Control	0.43 ± 0.24	103. 3 ± 4.48	32.95 ± 5.12	0.39 ± 0.17	3.81 ± 0.06
BTU	0.41 ± 0.21^{NS}	189.15 ± 8.84 ^{c}	42.13 ± 1.3^{b}	0.61 ± 0.11^{c}	4.29 ± 0.03^{a}
BTU + PL	0.49 ± 0.15^{NS}	100.46 ± 2.3^{NS**}	33.89 ± 1.35 ^{NS**}	0.46 ± 0.12^{NS*}	3.26 ± 0.61^{NS**}
BTU + IBU	0.47 ± 0.32 ^{NS**}	112.49 ± 3.9 ^{a***}	31.14 ± 4.7 ^{NS*}	0.52 ± 0.02 ^{a*}	3.47 ± 0.04 ^{NS}

Data are expressed as mean ± SD (n = 5). Statistical analysis was performed using one-way ANOVA followed by Tukey's post hoc test. $p < 0.05$ (), $p < 0.01$ (), and $p < 0.001$ () indicate significant differences compared with the BTU group, while NS denotes non-significant differences.

hepatoprotective and nephroprotective actions, which can be attributed to the extract's major polyphenols (caffeic acid, ferulic acid, rutin, myricetin (Basu Mallik et al., 2016). Comparable hepatoprotective effects were observed with *Cucurbita* seed extracts, which normalized serum AST, ALT, and renal markers in toxicological models (Bakeer, 2025). Ibuprofen (BTU + IBU) treatment also reduced AST to 112.49 ± 3.9 U/L ($p < 0.001$ vs. BTU) and normalized ALT (31.14 ± 4.7 U/L, NS) but was less effective than the extract in lowering urea (0.52 ± 0.02 g/L, $p < 0.05$) and creatinine (3.47 ± 0.04 mg/L), remained non-significant highlighting the broader multi-target protective effects of *C. maxima*. Similar superiority of phenolic-rich extracts over NSAIDs has been reported in other studies, where phenolic acids restored both hepatic enzymes and renal biomarkers more effectively than reference drugs (Alhoshani et al., 2017).

The restoration of hepatic and renal biomarkers following treatment with *C. maxima* leaf extract indicates a protective effect against BTU-induced organ injury. These improvements are consistent with attenuation of systemic inflammation and oxidative stress, processes commonly associated with dysregulation of NF-κB and antioxidant defense pathways (Liu and Lv, 2023; Y. Wang et al., 2025). Rather than reflecting a single molecular target, the observed effects likely result from the combined action of multiple polyphenolic constituents acting on interconnected inflammatory and redox-related mechanisms (Banjabi et al., 2025; Lu et al., 2025).

This reduction was more pronounced than that observed with ibuprofen, highlighting the potential of pumpkin-derived phytochemicals to effectively attenuate inflammation (Fig. 2).

3.2.3. Histopathological analysis

A) Liver Histology

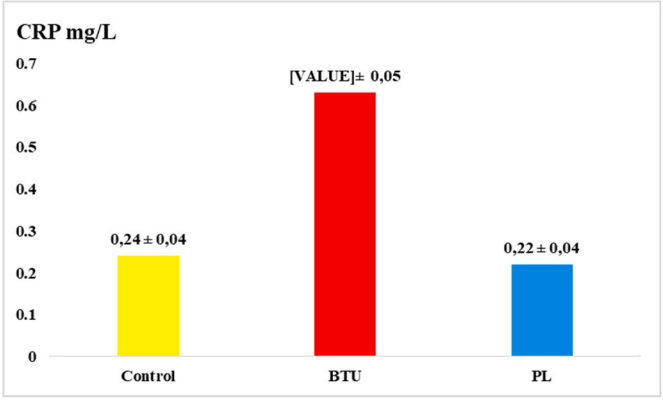

Fig. 2. Serum CRP levels in different groups (Control, BTU, Pumpkin Leaves) (5 animals per group).

In the BTU-treated group, liver sections revealed clear signs of hepatotoxicity, hepatocellular degeneration, necrosis, and inflammatory infiltration around the central veins and portal areas. Enlarged nuclei and irregular hepatic cords were also frequently observed (Fig. 3B). These microscopic lesions are fully consistent with the biochemical alterations observed, namely the significant elevations in AST and ALT, which reflect hepatocyte membrane rupture and leakage of cytosolic enzymes into circulation (Kizilirmak et al., 2022). The ibuprofen-treated group exhibited partial recovery, showing milder cellular degeneration and reduced congestion compared with the BTU group (Fig. 3C). In contrast, the control group displayed a typical hepatic lobular structure with well-organized hepatocytes radiating symmetrically around the central vein (Fig. 3A). Animals treated with *C. maxima* leaf extract (Fig. 3D) displayed nearly normal hepatic lobular architecture, with preserved hepatocyte organization and minimal inflammatory infiltration. This histological protection directly mirrors the normalization of AST and ALT values and the reduction of WBC and GRA toward control levels, indicating that the extract not only limited hepatocyte injury but also suppressed systemic and local immune cell activation. Ibuprofen produced partial recovery, but residual degeneration and congestion were still visible, whereas the extract yielded more complete restoration of hepatic architecture. These cross-level consistencies demonstrate that the hepatoprotective effect of *C. maxima* is both biochemically and histologically verifiable. Similar findings have been reported in other polyphenol-rich extracts: *Cucurbita* extract reduced hepatic lesions and improved transaminase profiles in toxin-induced hepatotoxicity (Abdalla et al., 2022; Enemali et al., 2018). Mechanistically, this protection can be attributed to abundant caffeic acid, ferulic acid, and rutin, which are known to inhibit NF-κB activation, downregulate COX-2/iNOS expression, and enhance endogenous antioxidant defenses, thereby reducing inflammatory cell infiltration and hepatocyte necrosis (Ma et al., 2024). In addition to these findings, it is crucial to highlight that the hepatoprotective effect of *C. maxima* corresponds with molecular mechanisms elucidated in alternative experimental hepatotoxicity models. Caffeic acid has been shown to activate the Nrf2/HO-1 pathway, which boosts the body's own antioxidant defenses, while at the same time blocking NF-κB signaling, which lowers the release of cytokines and hepatocellular necrosis [(Mahmoud et al., 2020). Ferulic acid also protects the liver by increasing the activity of antioxidant enzymes that are controlled by Nrf2 and decreasing the activity of pathways that are controlled by NF-κB and COX-2. This lowers oxidative stress and inflammation (Mahmoud et al., 2020) Rutin also protects the liver by raising the levels of GST, GPx, and SOD, turning on Nrf2/HO-1, and turning off iNOS and COX-2 expression. This gives the liver a multi-level defense (Rahmani et al., 2023).

Overall, the histopathological findings corroborate the biochemical and hematological data, supporting a protective role of *C. maxima* leaf extract against inflammation-associated tissue damage without reiterating pathway-level mechanisms already discussed.

B) Kidney's histology

The renal histopathological alterations observed in our BTU model vascular congestion (Fig. 4), tubular dilatation and necrosis, epithelial desquamation, and glomerular disorganization are in line with the lesions reported in experimental nephrotoxicity. Other models such as cisplatin and gentamicin reveal tubular necrosis, inflammation, and increased serum urea and creatinine. Nephroprotective interventions like flavonoid supplementation improve histology and biochemical indices, confirming the link between tissue injury and renal clearance markers (Huang et al., 2021; Mitra et al., 2025). The hematological profile in our study leukocytosis and elevated C-reactive protein (CRP) further substantiates the inflammatory dimension of renal injury. CRP has been implicated not only as a biomarker but also as an active mediator of renal inflammation and fibrosis, with experimental evidence linking CRP upregulation to tubular injury and progression of

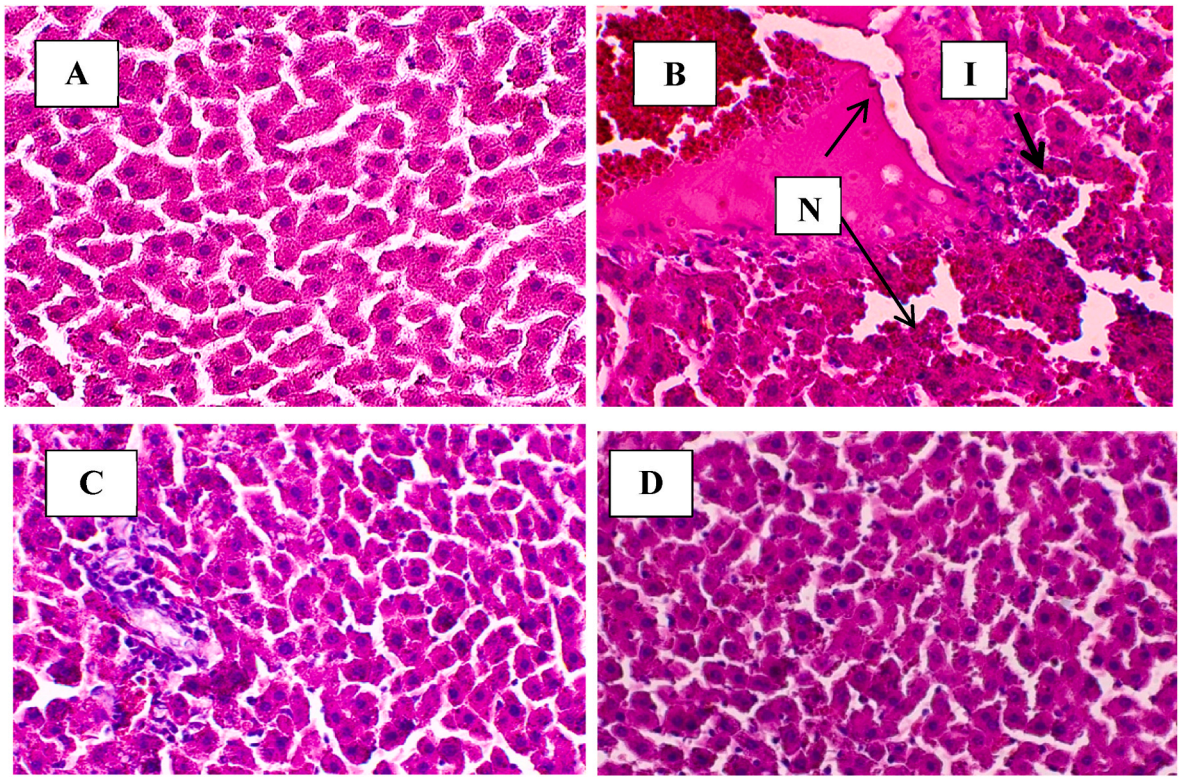

Fig. 3. Representative photomicrographs of liver sections stained with hematoxylin and eosin (H&E). (A) Control group showing normal hepatic lobular architecture with radiating hepatocytes. (B) BTU-treated group showing severe hepatocellular necrosis (N) and inflammatory infiltration (I) around central veins. (C) Ibuprofen-treated group showing partial recovery with reduced degeneration and congestion. (D) Pumpkin leaf extract–treated group showing nearly normal histoarchitecture with well-preserved hepatocyte organization. Magnification × 40. Each image is representative of 4 sections from 5 animals per group. Scale bar = 50 μm.

acute kidney injury (AKI)(Li et al., 2023).

The protective effect of *Cucurbita maxima* leaves may be attributed to its polyphenolic constituents, particularly caffeic acid and rutin. Caffeic acid has been shown to downregulate NF-κB and COX-2 signaling, thereby reducing oxidative stress and pro-inflammatory mediator release; in nephrotoxic models, this translated into preservation of tubular architecture and reduced fibrosis (Bencheikh et al., 2022). Likewise, rutin has been repeatedly demonstrated to attenuate cisplatin-induced nephrotoxicity by lowering creatinine, suppressing inflammatory cytokines, and ameliorating histopathological injury (Alhoshani et al., 2017). Complementary evidence from *Cucurbita* species supports this phytochemical-driven renoprotection, showing improvements in renal histoarchitecture and reductions in biochemical markers of kidney injury in toxicant-induced models (Y.-N. Wang et al., 2025).

The ibuprofen-treated group still showed prominent vascular congestion, though slightly less than BTU alone, suggesting limited protective effects. In contrast, co-treatment with leaf extracts significantly alleviated renal histopathological damage. These groups showed near-normal renal histoarchitecture, improved vascular conditions, and better preservation of tubular and glomerular structures, indicating the nephroprotective role of pumpkin components, possibly due to their anti-inflammatory properties (Radwan et al., 2023). There is substantial experimental evidence indicating that flavonoid-rich extracts and phenolic acids (such as ferulic acid) activate the Nrf2/HO-1 antioxidant pathway and suppress NF-κB/NLRP3-mediated inflammatory cascades, thus ameliorating tubular injury and reducing interstitial fibrosis in renal injury models. While extracts of *Cucurbita maxima* show promising nephroprotective effects, further mechanistic studies are needed to confirm activation of these specific pathways in that model (Enemali et al., 2018; Jiang et al., 2024).

Rutin has demonstrated the ability to safeguard the kidneys from cisplatin-induced damage by reducing serum creatinine and urea concentrations, inhibiting pro-inflammatory cytokines, and enhancing the architecture of the glomeruli and tubules (Alhoshani et al., 2017).

The decrease in CRP levels noted in our study offers a dual advantage: alleviation of acute inflammation and inhibition of long-term fibrotic progression, as CRP upregulation is directly associated with tubular injury and the progression from acute kidney injury (AKI) to chronic kidney disease. These findings suggest that the nephroprotective effects of *C. maxima* surpass its antioxidant properties, encompassing intricate modulation of cellular defense mechanisms, inflammatory pathways, and fibrosis-related signaling. This extensive protection clarifies the nearly total restoration of renal architecture in extract-treated animals and emphasizes the translational potential of *C. maxima* as an adjunctive therapeutic candidate for drug-induced nephrotoxicity.

3.3. *In vitro anti-inflammatory activity*

The protein denaturation inhibition assay demonstrated that the aqueous leaf extract *of Cucurbita maxima* displays concentration-dependent anti-inflammatory activity, as indicated by a gradual increase in the percentage of inhibition with higher doses. The extract had an IC_{50} value of 2.976 mg/mL, which meant it was biologically active. However, it wasn't as strong as diclofenac (IC_{50} = 0.718 mg/mL), a well-known drug that strongly stops COX-1 and COX-2 enzymes (Rastogi et al., 2018) (Table 4; Fig. 5).

The extract has a lot of bioactive compounds, such as phenols, flavonoids, and saponins, which is why it works. These compounds are well-known for their ability to stop inflammatory pathways by blocking COX, lowering the production of prostaglandins, and protecting proteins from damage caused by free radicals (Middleton et al., 2000). It is also likely that the extract contributes to the regulation of pro-inflammatory

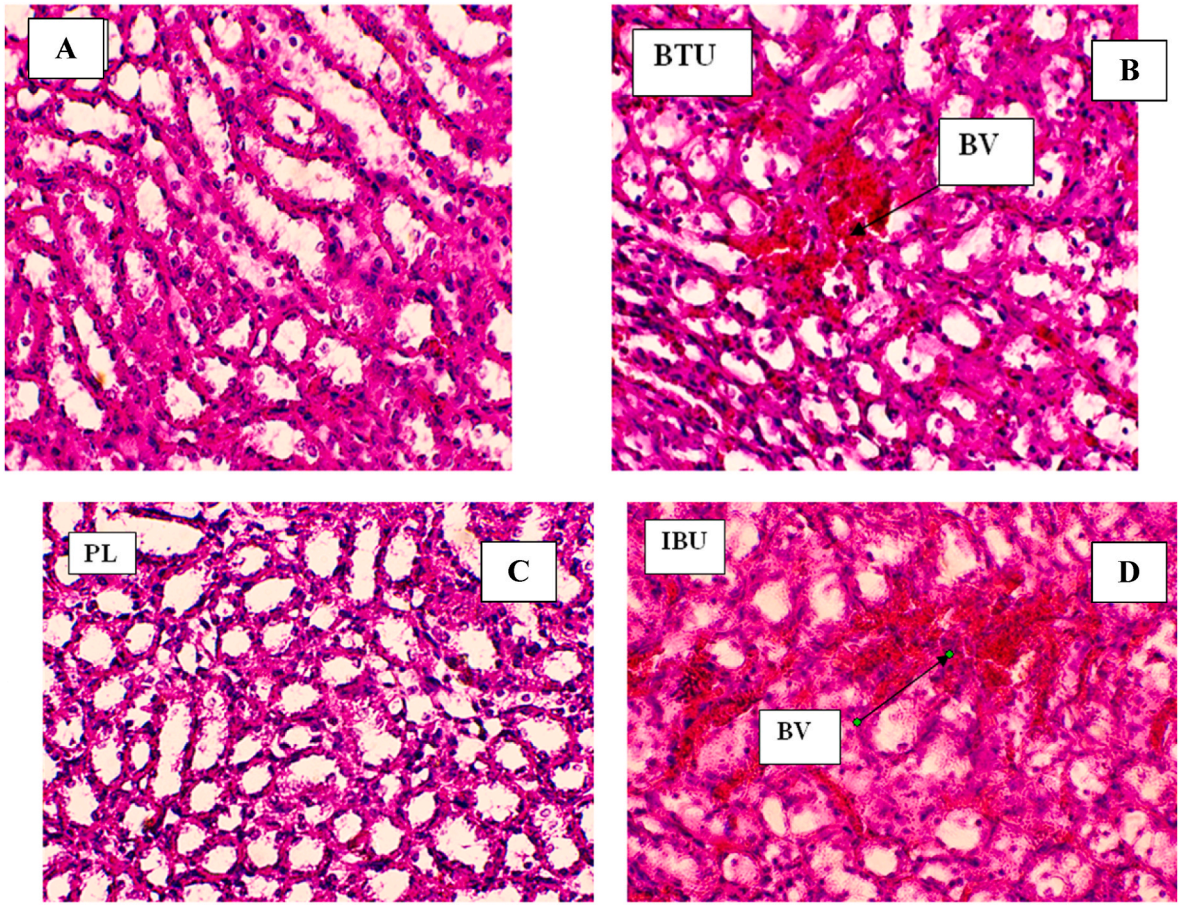

Fig. 4. Representative photomicrographs of kidney sections stained with hematoxylin and eosin (H&E). (A) Pumpkin leaf extract–treated group showing preserved renal histoarchitecture with intact glomeruli and tubules. (B) Ibuprofen-treated group showing moderate vascular congestion (BV). (C) Control group displaying normal renal architecture. (D) BTU-treated group showing severe vascular congestion (BV), tubular dilation, and disorganized glomeruli. Magnification × 40. Images are representative of four sections per kidney from eight rats per group. Scale bar = 50 μm.

cytokines such as TNF-α and IL-1β, thus providing a multi-level mechanism that reinforces its anti-inflammatory effect (Balgoon et al., 2021).

These results indicate a measurable anti-inflammatory activity of the extract in the protein denaturation model; however, its potency remains lower than that of diclofenac, a standard nonsteroidal anti-inflammatory drug.

It should be emphasized that the protein denaturation assay is a non-specific in vitro model that provides indirect evidence of anti-inflammatory potential. While it is useful for preliminary screening, it does not directly reflect inhibition of specific inflammatory mediators or signaling pathways. Therefore, the observed activity should be interpreted with caution and considered as supportive rather than definitive evidence of anti-inflammatory efficacy.

3.4. *In silico study*

3.4.1. *Molecular docking analysis of C. maxima phytochemicals*

To elucidate the molecular interactions underlying the pharmacological potential of *C. maxima*, molecular docking simulations were performed on its major phytochemicals (≥1% abundance in leaf extracts). The selected compounds included Kojic Acid (KJA, 0.97%), Oleuropein (OLP, 0.98%), Chrysin-6-C-glucoside (C6G, 1.01%), p-Coumaric Acid (PCA, 1.47%), Salicylic Acid (SLA, 2.07%), Myricetin (MYR, 2.49%), Quercetin-3-glucoside (Q3G, 3.04%), Catechin (−) (CAT, 3.67%), Riboflavin (RBF, 7.29%), Hispidulin (HSD, 7.88%), Sinapic Acid (SNA, 8.60%), Myricetin-3-rhamnose (M3R, 8.62%), Ferulic Acid (FEA, 8.79%), Rutin (RTN, 9.25%), and Caffeic Acid (CFA, 56.04%). Diclofenac (DIF) was included as a reference drug. The docking was conducted against three key proteins: serum albumin (BSA; PDB ID: 6QS9), cyclooxygenase-1 (COX-1; PDB ID: 1EQG), and cyclooxygenase-2 (COX-2; PDB ID: 1PXX), which are directly implicated in drug transport and inflammatory regulation.

Validation of the docking protocol was achieved by redocking the co-crystallized native ligands into their respective binding sites, followed by root-mean-square deviation (RMSD) analysis. All RMSD values were below the accepted threshold of 2.0 Å(T. Lanez and Lanez, 2016), confirming the reliability and reproducibility of the docking procedure. Notably, RMSD values were 0.603 Å for COX-1, 0.991 Å for COX-2, and 1.778 Å for BSA, indicating robust docking parameters (Fig. 6; Table 5).

Several phytoconstituents exhibited strong predicted binding affinities, in some cases comparable to those of the native ligands and the reference drug. These results suggest a favorable interaction potential with inflammatory targets; however, they represent in silico predictions that require experimental validation to confirm functional enzyme inhibition. Among these, M3R demonstrated the strongest affinities toward COX-2 (−9.60 kcal/mol) and BSA (−8.66 kcal/mol), surpassing both the native ligands and the reference drug. In contrast, its relatively low affinity for COX-1 (−5.08 kcal/mol) suggests a selective preference for COX-2, highlighting its potential as a targeted anti-inflammatory agent.

Similarly, C6G, RBF, Q3G, HSD, CAT, and MYR displayed strong interactions with COX-2 (−9.33 to −7.99 kcal/mol), outperforming the native ligand (−7.99 kcal/mol) and the reference drug DIF (−7.91 kcal/mol). This reinforces their involvement in anti-inflammatory

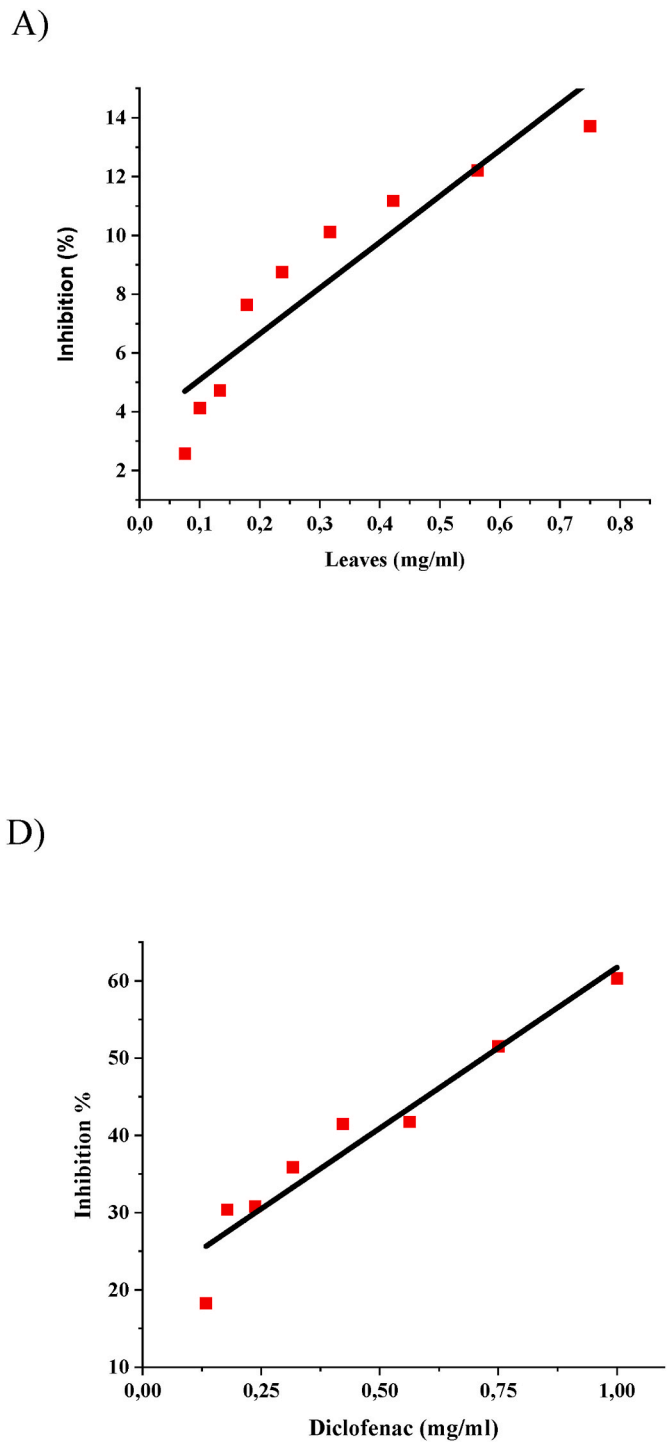

Fig. 5. Exponential regression curves of anti-inflammatory percentage inhibition versus concentration of (A) leaf extract and (D) Diclofenac.

Table 4
Absorbance values taken from the anti-inflammatory test.

	Slope	Intercept	R^2	IC_{50} (mg/mL)
Leaves	15.616	3.526	0.862	2.976
Diclofenac	41.669	20.074	0.913	0.718

mechanisms mediated through COX-2 inhibition. With COX-1, compounds such as HSD, CAT, MYR, and Q3G maintained binding affinities ranging from −7.85 to −7.24 kcal/mol, values comparable to the native ligand (−7.26 kcal/mol) though slightly lower than DIF (−8.41 kcal/mol).

Furthermore, compounds including MYR, RBF, Q3G, CAT, HSD, and OLP exhibited strong binding toward BSA (−7.99 to −7.20 kcal/mol), with affinities comparable to DIF (−7.07 kcal/mol), suggesting a favorable interaction profile that could facilitate transport and bioavailability in vivo.

In contrast, weaker affinities were recorded for CFA (−5.42 to −5.39), PCA (−5.32 to −5.10), FEA (−5.92 to −5.51), KJA (−4.83 to −4.54), RTN (−7.19 to −3.32), SLA (−4.37 to −4.23), and SNA (−5.99 to −5.87) against the three target proteins, indicating a more limited direct role in molecular interactions. Nevertheless, the predominance of CFA (56.04%) in the extract, despite its moderate binding affinity, suggests that its high abundance may contribute synergistically alongside other potent compounds (Ali et al., 2024; Khan et al., 2021).

Collectively, these results suggest that multiple phytochemicals in *C. maxima* act synergistically through stable interactions with COX-1, COX-2, and BSA, supporting the experimentally observed anti-inflammatory and pharmacological potential of the extract. Among them, seven compounds (M3R, C6G, RBF, Q3G, HSD, CAT, and MYR) emerged as the most promising lead candidates. Their consistently strong binding affinities, favorable interaction profiles, and structural complementarity with the target proteins highlight their potential as multi-target modulators of inflammatory pathways. These findings provide a rational basis for prioritizing these phytoconstituents in future in vitro and in vivo validation studies, as well as in structure-based drug design efforts aimed at developing novel anti-inflammatory therapeutics.

The native ligand (NL) of COX-2 (1PXX) established three hydrogen bonds with Arg89, Tyr324, and Val492, in addition to extensive hydrophobic contacts with Val318, Leu321, Leu353, Tyr354, Trp356, Phe487, Met491, Gly495, Ala496, Ser499, and Leu500. In comparison, diclofenac (DIF) engaged in two hydrogen bonds (Arg89, Tyr324) and displayed hydrophobic interactions with Leu321, Ser322, Tyr354, Trp356, Val492, Gly495, Ala496, and Ser499 (Fig. 7). All lead phytoconstituents docked into the COX-2 active site showed hydrogen bonding with residues shared by the native ligand. M3R exhibited the strongest polar network, forming eight hydrogen bonds with Arg89, Leu321, Tyr324, Tyr354, and Ser499. C6G formed four hydrogen bonds with Arg89, Tyr324, Val492, and Ala496. Similarly, Q3G, RBF, nd MYR each established five hydrogen bonds: Q3G with Arg89, Tyr324, Phe487, and Ser499; RBF with Arg89, Met491, Val492, and Ala496; and MYR with His58, Ser322, Gln161, and Met491 (Fig. S1). HSD formed three hydrogen bonds with His58, Ser322, and Tyr324, while CAT established two with Ser499 (Fig. S1). These conserved interactions highlight the ability of *C. maxima* flavonoids to anchor within the COX-2 active site via critical residues involved in NSAID binding.

The native ligand (NL) of COX-1 (1EQG) interacted through three hydrogen bonds with Arg88 and Tyr323, stabilized by hydrophobic residues Val84, Val317, Trp355, Phe486, Met490, Ile491, Gly494, Ala495, and Leu499. In contrast, DIF engaged in a single hydrogen bond with Ala495, supported by hydrophobic contacts with Val317, Leu320, Ser321, Phe349, Leu352, Tyr353, Trp355, Met490, Gly494, Ser498, and Leu499 (Fig. 8).

Similarly, all lead compounds displayed hydrogen bonding with key residues of the native ligand. CAT and MYR both formed three hydrogen bonds with Arg88, Tyr323, and Met490 (Fig. 8, Fig. S2). HSD and C6G engaged in two to three hydrogen bonds with Arg88 and Tyr323 (Fig. 8). Q3G established four hydrogen bonds with Arg88, Tyr353, Met490, and Ser498 (Fig. S2). The docking results are discussed here in terms of predicted binding interactions and structural complementarity only, without reiterating downstream inflammatory pathways already addressed in the experimental sections.

3.4.2. ADMET and drug-likeness prediction for phytochemical constituents

ADMET predictions were used to obtain a preliminary assessment of

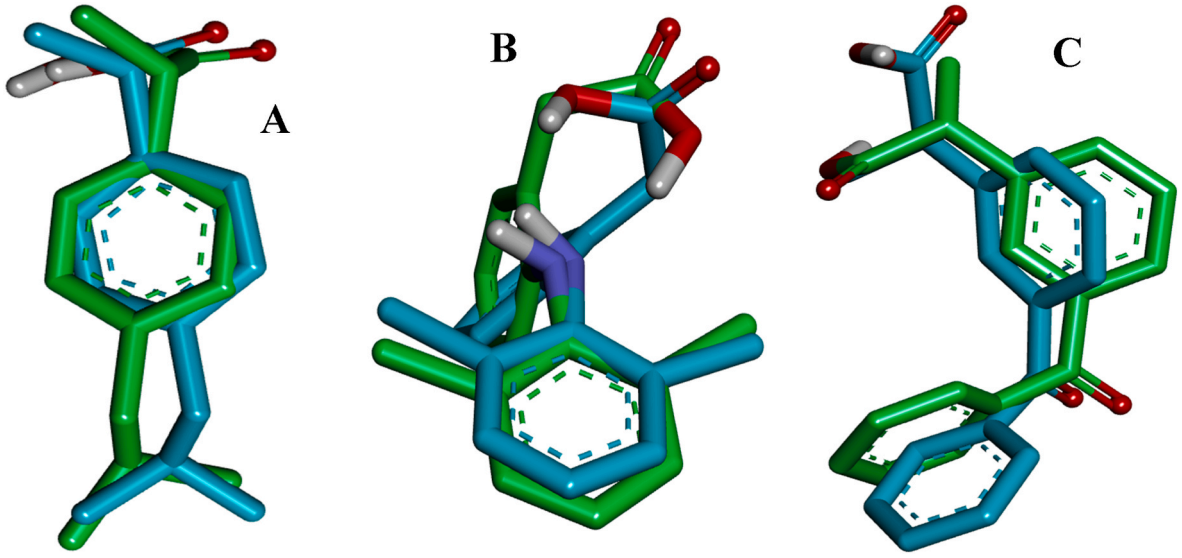

Fig. 6. Superimposed docking poses showing native ligand (green) and redocked conformation (blue) in the active site of (A) COX-1 (1EQG); (B) COX-2 (1PXX); and (C) BSA (6QS9). (For interpretation of the references to colour in this figure legend, the reader is referred to the Web version of this article.)

Table 5
Binding energies (kcal/mol) of *C. maxima* phytochemicals and reference drug against COX-1 (1EQG), COX-2 (1PXX), and BSA (6QS9).

	1EQG	1PXX	6QS9
RMSD Å	**0.603**	**0.991**	**1.778**
Native ligand	−7.29	−7.99	−8.05
DIF	−8.41	−7.91	−7.07
CFA	−5.39	−5.30	−5.42
CAT	**−7.75**	**−8.22**	−7.42
C6G	**−7.49**	**−9.33**	−6.50
PCA	−5.10	−5.14	−5.32
FEA	−5.92	−5.51	−5.52
HSD	**−7.85**	**−8.68**	−7.20
KJA	−4.54	−4.46	−4.83
M3R	−5.08	**−9.60**	−8.66
MYR	**−7.35**	**−7.99**	−7.94
OLP	−3.36	−6.70	−7.99
Q3G	**−7.24**	**−8.82**	−7.60
RBF	−6.01	**−8.85**	−7.72
RTN	−3.32	−7.19	−5.41
SLA	−4.37	−4.25	−4.23
SNA	−5.87	−5.99	−5.61

the pharmacokinetic behavior and safety of the major phytochemicals identified in *C. maxima* leaves (Table 6). Among the evaluated compounds, catechin (CAT), chrysin-6-C-glucoside (C6G), and hispidulin (HSD) showed the most favorable profiles, combining acceptable solubility, high predicted gastrointestinal absorption, limited CYP inhibition liability, and satisfactory clearance values (Laraoui et al., 2023). Other compounds, such as myricetin-3-rhamnose (M3R), quercetin-3-glucoside (Q3G), and riboflavin (RBF), exhibited reduced oral absorption or multiple drug-likeness rule violations, suggesting that formulation strategies or structural optimization may be required to enhance their developability (E. Lanez et al., 2023). Overall, the ADMET analysis supports the potential of selected *C. maxima* phytochemicals as orally relevant candidates, while emphasizing the need for experimental pharmacokinetic validation.

The toxicity profile of the *C. maxima* lead compounds is generally favorable, supporting their potential as safe therapeutic agents (Table 7). Among them, Q3G and MYR exhibited the highest LD_{50} values (5.052 and 3.898 mol/kg, respectively), suggesting relatively low acute toxicity. RBF (3.392 mol/kg), M3R (2.537 mol/kg), HSD (2.482 mol/kg), CAT (2.428 mol/kg), and C6G (2.261 mol/kg) showed comparatively lower LD_{50} values but still indicate acceptable safety margins.

Regarding mutagenicity, all compounds were predicted to be non-mutagenic in the Ames test except HSD, which showed a positive result. For cardiotoxicity, only M3R was flagged as a potential hERG I inhibitor, warranting further investigation. Importantly, none of the compounds were predicted to be hepatotoxic or skin sensitizers, emphasizing their overall favorable safety profile (Mouada et al., 2025).

Taken together, these findings indicate that the *C. maxima* lead compounds are characterized by low acute toxicity and minimal organ-specific risks, with Q3G and MYR standing out as particularly safe candidates for further pharmaceutical development.

4. Conclusion

This research provides a solid foundation for further exploring *Cucurbita maxima* leaf extract as a source of bioactive phytochemical combinations with anti-inflammatory potential, while recognizing that the activity of the crude extract may differ from that of isolated individual constituents due to synergistic effects. By integrating detailed phytochemical analysis with rigorous in vitro and in vivo evaluations, the research reveals the molecular and pharmacological basis of the extract's therapeutic effects.

The extract contains a rich array of bioactive polyphenols chiefly gallic acid, ellagic acid, luteolin, apigenin, and rutin that synergistically inhibit key inflammatory mediators, including cyclooxygenase-2 (COX-2), inducible nitric oxide synthase (iNOS), and NF-κB signaling pathways. Notably, the extract demonstrated superior inhibition of protein denaturation in vitro, outperforming the standard NSAID diclofenac and underscoring its strong biochemical anti-inflammatory potential.

In animal models, the extract effectively mitigated benzylthiouracil-induced systemic inflammation by normalizing hematological parameters, markedly reducing circulating C-reactive protein levels, and protecting liver and kidney tissues from inflammation-induced damage. Histopathological analysis confirmed near-complete preservation of tissue architecture following treatment.

Molecular docking results support these findings by showing that the lead flavonoids (M3R, C6G, RBF, Q3G, HSD, CAT, and MYR) exhibit strong and stable binding to COX-1 and COX-2, in some cases surpassing the native ligands and diclofenac. These interactions, characterized by stable hydrogen bonds and hydrophobic contacts within the catalytic pockets, highlight their direct modulatory role on inflammatory

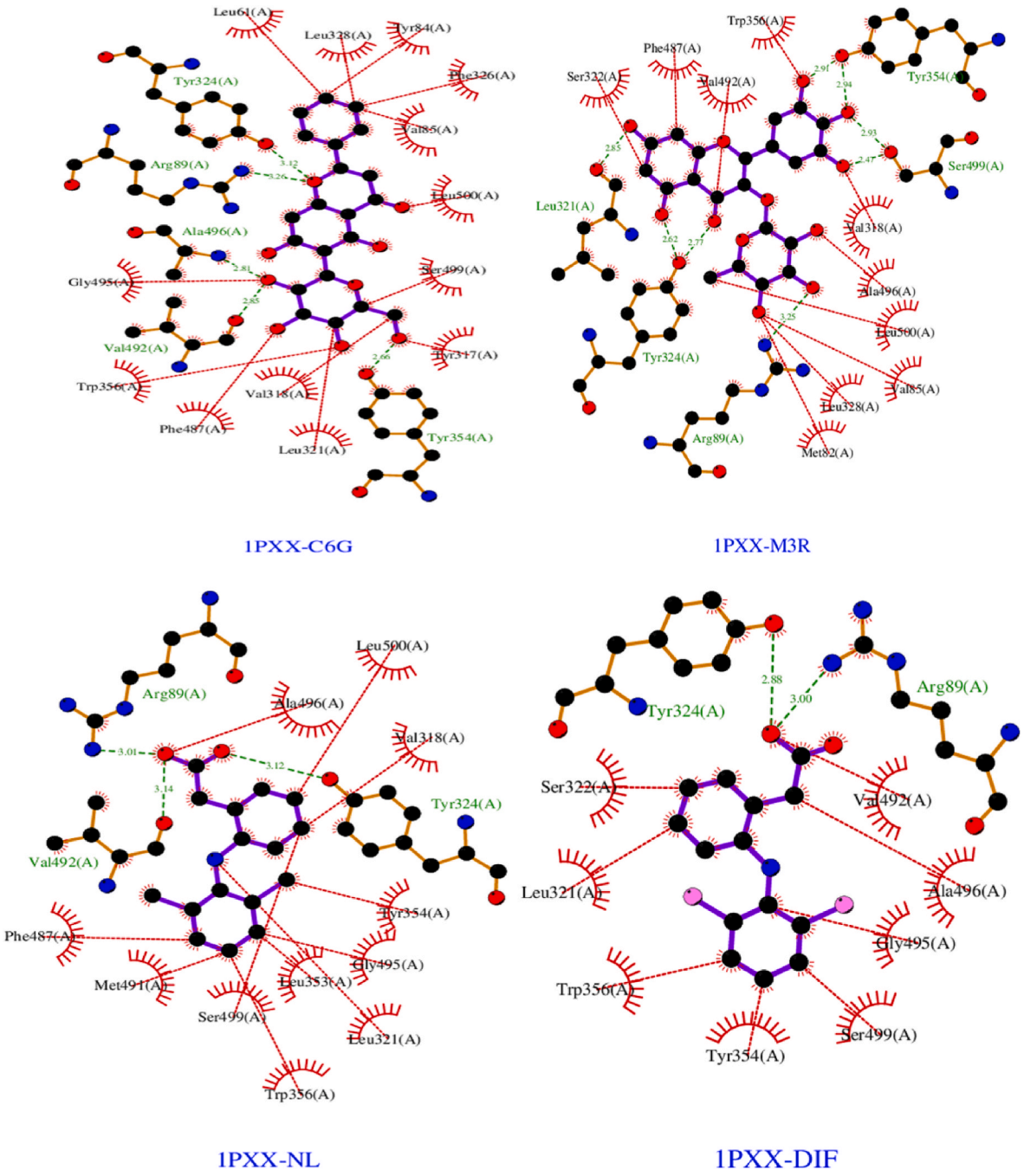

Fig. 7. Binding interactions of C6G, M3R, DIF and NL within the active site of COX-2.

enzymes. ADME and toxicity predictions further supported their favorable pharmacokinetic and safety profiles, with Q3G and MYR emerging as particularly promising drug-like candidates.

Overall, this study validates the traditional medicinal use of *Cucurbita maxima* and highlights its potential as a natural, safe, and effective alternative to conventional anti-inflammatory drugs, which often carry undesirable side effects. A limitation of the present study is that the in vitro anti-inflammatory evaluation was restricted to the protein denaturation assay. The absence of complementary mechanistic assays, such as cyclooxygenase inhibition, nitric oxide suppression, or pro-inflammatory cytokine (TNF-α, IL-1β) measurements, limits the direct assessment of molecular targets. Future studies incorporating these assays are warranted to further substantiate the anti-inflammatory mechanisms of *Cucurbita maxima* leaf extract. Future work should focus on isolating and characterizing individual active compounds, clarifying their molecular targets, and conducting comprehensive clinical evaluations to fully realize their therapeutic potential. This research provides a solid foundation for advancing *Cucurbita maxima* as a novel source of plant-based anti-inflammatory agents, contributing to the development of safer, multi-target phototherapeutics in modern medicine. It should be noted that benzylthiouracil is not a conventional acute inflammation model, such as carrageenan or lipopolysaccharide-induced inflammation. Therefore, the anti-inflammatory effects observed in this study reflect modulation of systemic and organ-associated inflammation secondary to BTU-induced metabolic and immune disturbances. This limitation should be considered when extrapolating the findings, and future studies employing classical inflammatory models are warranted to further validate the anti-

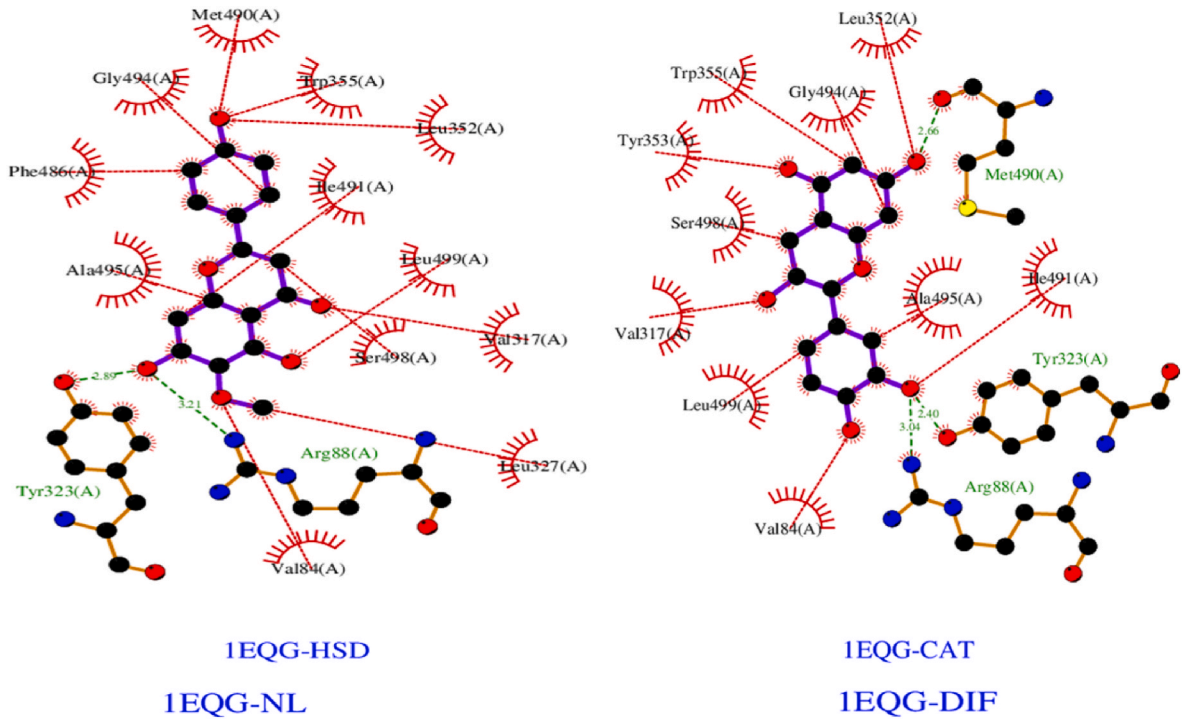

Fig. 8. Binding interactions of HSD, CAT, DIF and NL within the active site of COX-1.

Table 6
Predicted pharmacokinetic and drug-likeness properties of *C. maxima* lead.

Compounds	CAT	C6G	HSD	M3R	MYR	Q3G	RBF
Log S (ESOL)	−2.22	−2.97	−3.99	−3.20	−3.01	−3.03	−1.31
Caco-2 permeability (log Papp in 10^{-6} cm/s)	2.514	3.555	−0.045	−0.982	0.095	−2.231	−0.679
GI absorption (%)	85.174	81.669	84.654	43.334	65.93	0	36.107
P-gp substrate	Yes	NO	Yes	Yes	No	No	No
VDss (log L/kg)	0.011	0.011	0.37	1.552	1.317	0.011	−0.196
CYP1A2 inhibitor	No	NO	Yes	No	Yes	No	No
CYP2C19 inhibitor	No	No	No	No	No	No	No
CYP2C9 inhibitor	No	No	No	No	No	No	No
CYP2D6 inhibitor	No	No	Yes	No	No	No	No
CYP3A4 inhibitor	No	No	Yes	No	Yes	No	No
Total Clearance (log ml/min/kg)	−30.053	−23.47	0.531	0.303	0.422	−44.694	0.7
Renal OCT2 substrate	No	No	No	No	No	No	No
Lipinski	Yes 0 V	Yes 1 V	Yes 0 V	No 2 V	Yes 1 V	No 2 V	Yes 0 V
Ghose	Yes	Yes	Yes	Yes	Yes	Yes	No 1 V
Veber	Yes	No 1 V	Yes	No 1 V	No 1 V	No 1 V	No 1 V
Egan	Yes	No 1 V	Yes	No 1 V	No 1 V	No 1 V	No 1 V
Muegge	YES	No 2 V	Yes	No 3 V	No 2 V	No 3 V	No 1 V
BAS	0.55	0.55	0.55	0.17	0.55	0.11	0.55

Abbreviations: CAT, catechin; C6G, chrysin-6-C-glucoside; HSD, hispidulin; M3R, myricetin-3-rhamnose; MYR, myricetin; Q3G, quercetin-3-glucoside; RBF, riboflavin.

Table 7
Toxicity prediction of Lead Compounds of *C. maxima*.

	CAT	C6G	HSD	M3R	MYR	Q3G	RBF
LD_{50} (mol/kg)	2.428	2.261	2.482	2.537	3.898	5.052	3.392
AMES	No	No	Yes	No	No	No	No
hERG I inhibitor	No	No	No	Yes	No	No	No
Hepatotoxicity	No	No	No	No	No	No	No
Skin Sensitization	No	No	No	No	No	No	No

inflammatory potential of *Cucurbita maxima*.

CRediT authorship contribution statement

Hammadi Maroua: Investigation, Formal analysis, Data curation. **Mohammed Larbi Benamor:** Validation, Resources, Methodology. **Yahia Bekkar:** Writing – review & editing, Writing – original draft, Validation, Software, Investigation, Formal analysis, Conceptualization. **Salah Neghmouche Nacer:** Writing – review & editing, Supervision, Resources, Project administration, Methodology. **Elhafnaoui Lanez:** Software, Investigation, Data curation. **Ouafa Boudebia:** Visualization, Validation, Methodology. **Housseyn Chaoua:** Investigation, Data

curation. **Aicha Adaika:** Validation, Resources, Methodology. **Lazhar Bechki:** Visualization, Software, Formal analysis. **Touhami Lanez:** Writing – review & editing, Supervision, Project administration, Conceptualization. **Stefania Garzoli:** Writing – review & editing, Supervision.

Ethics approval

All experimental procedures involving animals were conducted in accordance with the international guidelines for the care and use of laboratory animals and were approved by the Scientific Council Committee of the Faculty of Natural Sciences and Life, University of El Oued. The study was carried out under ethical approval reference number: 29/S.C/F.l.N.S/E.U/2025.

Funding declaration

This research did not receive any specific grant from funding agencies in the public, commercial, or not-for-profit sectors.

Declaration of competing interest

The authors declare that they have no known competing financial interests or personal relationships that could have appeared to influence the work reported in this paper.

Acknowledgments

This work was supported by the directorate-general of scientific research and technological development (DGRSDT) and the laboratory of valorization and technology of Saharan resources (VTRS) (project code: B00L01UN390120150001).

Appendix A. Supplementary data

Supplementary data to this article can be found online at https://doi.org/10.1016/j.jep.2026.121267.

Data availability

Data will be made available on request.

References

Abdalla, O., Hashem, M., Abdelnaeim, N., Elazouney, D., 2022. Hepatoprotective effects of Moringa Oleifera seed oil and pumpkin seed oil on CCL4 induced hepatotoxicity in rats. Suez Canal Veterinary Medical Journal. SCVMJ 27 (2), 315–331. https://doi.org/10.21608/scvmj.2022.281309.

Adaika, A., Bekkar, Y., Youmbai, S., Bourougaa, L., Lanez, E., Larbi, B.A., Nesba, K., Lanez, T., Bechki, L., 2025. Synthesis, antioxidant, and antidiabetic potential of ferrocenylmethylnucleobase compounds: in vitro, in silico molecular docking, DFT calculation, and molecular dynamic simulations. Appl. Organomet. Chem. 39. https://doi.org/10.1002/aoc.7988.

Alhoshani, A.R., Hafez, M.M., Husain, S., Al-Sheikh, A.M., Alotaibi, M.R., Al Rejaie, S.S., Alshammari, M.A., Almutairi, M.M., Al-Shabanah, O.A., 2017. Protective effect of rutin supplementation against cisplatin-induced nephrotoxicity in rats. BMC Nephrol. 18 (1), 194. https://doi.org/10.1186/s12882-017-0601-y.

Ali, W., Choe, K., Park, J.S., Ahmad, R., Park, H.Y., Kang, M.H., Park, T.J., Kim, M.O., 2024. Kojic acid reverses LPS-induced neuroinflammation and cognitive impairment by regulating the TLR4/NF-κB signaling pathway. Front. Pharmacol. 15, 1443552. https://doi.org/10.3389/fphar.2024.1443552.

Alqahtani, S., 2017. In silico ADME-Tox modeling: progress and prospects. Expert Opin. Drug Metab. Toxicol. 13 (11), 1147–1158. https://doi.org/10.1080/17425255.2017.1389897.

Altaf, A., Sharma, H., Dar, A.H., Dash, K.K., Pandey, V.K., Manzoor, M., 2025. Phytochemical potential and biological activity of pumpkin: a review. Food Safety and Health 3 (2), 188–201. https://doi.org/10.1002/fsh3.70001.

Amrouche, B., Benyoucef, A., Kara, K., Aissa, C., Karamostefa, C., 2020. New intelligent fault diagnosis (IFD) approach for grid-connected photovoltaic systems. Energy 211, 118591. https://doi.org/10.1016/j.energy.2020.118591.

Araújo, L.S., Torquato, B.G.S., da Silva, C.A., Dos Reis Monteiro, M.L.G., Dos Santos Martins, A.L.M., da Silva, M.V., Dos Reis, M.A., Machado, J.R., 2020. Renal expression of cytokines and chemokines in diabetic nephropathy. BMC Nephrol. 21 (1), 308. https://doi.org/10.1186/s12882-020-01960-0.

Arjumand, W., Seth, A., Sultana, S., 2011. Rutin attenuates cisplatin induced renal inflammation and apoptosis by reducing NFκB, TNF-α and caspase-3 expression in wistar rats. Food Chem. Toxicol. : An International Journal Published for the British Industrial Biological Research Association 49 (9), 2013–2021. https://doi.org/10.1016/j.fct.2011.05.012.

Bakeer, M.R., 2025. Detection of the ameliorative and antioxidant effects of pumpkin seed oil and olive oil on DBP-induced nephrotoxicity in Male albino rats by investigating their protective properties on physiological and histological measures. Egypt. J. Vet. Sci. 1–12. https://doi.org/10.21608/ejvs.2025.340222.2527.

Balgoon, M.J., Al-Zahrani, M.H., Jaouni, S. Al, Ayuob, N., 2021. Combined oral and topical application of pumpkin (Cucurbita pepo L.) alleviates contact dermatitis associated with depression through downregulation pro-inflammatory cytokines. Front. Pharmacol. 12 (May), 1–13. https://doi.org/10.3389/fphar.2021.663417.

Banjabi, A., Khalifa, F., Al-Bazi, M., Alkhodair, S., Al Doghaither, H., Sabban, A., Aljahdali, S., Albishi, H., 2025. Promising hepatorenal protective effects of pumpkin (Cucurbita pepo L.) and watermelon (Citrullus lanatus L.) seed oils against diazinon-induced acute toxicity in rats. Annals of Clinical and Analytical Medicine 16. https://doi.org/10.4328/ACAM.22439.

Basu Mallik, S., Mudgal, J., Nampoothiri, M., Hall, S., Dukie, S.A.-, Grant, G., Rao, C.M., Arora, D., 2016. Caffeic acid attenuates lipopolysaccharide-induced sickness behaviour and neuroinflammation in mice. Neurosci. Lett. 632, 218–223. https://doi.org/10.1016/j.neulet.2016.08.044.

Bekkar, Y., Saada, Z., Benine, A., 2025. Computational Analysis of N-ferrocenylmethyl-N-phenylbenzohydrazide: Molecular Docking and Dynamic Stability with BSA, vol. 1, pp. 29–43.

Bencheikh, N., Ouahhoud, S., Cordero, M.A.W., Alotaibi, A., Fakchich, J., Ouassou, H., Assri, S. El, Choukri, M., Elachouri, M., 2022. Nephroprotective and Antioxidant Effects of Flavonoid-Rich Extract of Thymelaea microphylla Coss. et Dur Aerial Part. Appl. Sci. 12 (18). https://doi.org/10.3390/app12189272.

Berman, H.M., Westbrook, J., Feng, Z., Gilliland, G., Bhat, T.N., Weissig, H., Shindyalov, I.N., Bourne, P.E., 2000. The protein data bank. Nucleic Acids Res. 28 (1), 235–242. https://doi.org/10.1093/nar/28.1.235.

Calixto, J.B., 2019. The role of natural products in modern drug discovery. An. Acad. Bras. Cienc. 91 (Suppl. 3), e20190105. https://doi.org/10.1590/0001-3765201920190105.

Daina, A., Michielin, O., Zoete, V., 2017. SwissADME: a free web tool to evaluate pharmacokinetics, drug-likeness and medicinal chemistry friendliness of small molecules. Sci. Rep. 7, 42717. https://doi.org/10.1038/srep42717.

Dhorajiwala, T., Halder, S., Samant, L., 2019. Comparative in silico molecular docking analysis of L-Threonine-3-Dehydrogenase, a protein target against African trypanosomiasis using selected phytochemicals. Biotechnol. Rep. https://doi.org/10.29252/JABR.06.03.04.

Diemar, M.G., Krul, C.A.M., Teunis, M., Busquet, F., Kandarova, H., Zajac, J.D., Vinken, M., Roggen, E.L., 2025. Report of the first ONTOX hackathon: hack to save lives and avoid animal suffering. The use of artificial intelligence in toxicology - a potential driver for reducing/replacing laboratory animals in the future. Altern. Lab. Anim. : ATLA 53 (1), 42–61. https://doi.org/10.1177/02611929241305112.

Donate-Correa, J., Ferri, C.M., Sánchez-Quintana, F., Pérez-Castro, A., González-Luis, A., Martín-Núñez, E., Mora-Fernández, C., Navarro-González, J.F., 2020. Inflammatory cytokines in diabetic kidney disease: Pathophysiologic and therapeutic implications. Front. Med. 7, 628289. https://doi.org/10.3389/fmed.2020.628289.

Duistermaat, J.J., Kolk, J.A.C., 2000. Proper actions. In: Lie Groups. Springer Berlin Heidelberg, pp. 93–130. https://doi.org/10.1007/978-3-642-56936-4_2.

Eberhardt, J., Santos-Martins, D., Tillack, A.F., Forli, S., 2021. AutoDock vina 1.2.0: new docking methods, expanded force field, and python bindings. J. Chem. Inf. Model. 61 (8), 3891–3898. https://doi.org/10.1021/acs.jcim.1c00203.

Elhewehy, A.A., El-fishawy, A.M., El-Rashedy, A.A., Fayez, A.M., Fayed, M.A.A., Mohsen, E., 2025. UPLC-ESI–MS/MS phytochemical profile, in vitro, in vivo, and in silico anti-alzheimer's activity assessment of Pithecellobium dulce (Roxb.) Benth. leaves. Future J. Pharmaceut. Sci. 11 (1), 30. https://doi.org/10.1186/s43094-025-00776-9.

Enemali, M., Bamidele, T., Ubana, M., 2018. Protective effect of ethanolic extract of Cucurbita maxima (PUMPKIN) leaf on acetaminophen-induced acute liver toxicity. J. Pharmacogn. Phytotherapy 10, 142–148. https://doi.org/10.5897/JPP2018.0498.

Ertas, A., Yener, I., 2020. A comprehensive study on chemical and biological profiles of three herbal teas in Anatolia; rosmarinic and chlorogenic acids. South Afr. J. Bot. 130, 274–281. https://doi.org/10.1016/j.sajb.2020.01.008.

Farkouh, A., Hemetsberger, M., Noe, C.R., Baumgärtel, C., 2022. Interpreting the benefit and risk data in between-drug comparisons: illustration of the challenges using the example of mefenamic acid versus ibuprofen. Pharmaceutics 14 (10). https://doi.org/10.3390/pharmaceutics14102240.

Ha, J., Kim, H., 2006. Caffeic acid phenethyl ester inhibits osteoclastogenesis through suppression of NF-kappaB, NFATc1, and c-Fos. Mol. Biol. Cell 17.
Huang, C.-W., Lee, S.-Y., Wei, T.-T., Kuo, Y.-H., Wu, S.-T., Ku, H.-C., 2021. A novel caffeic acid derivative prevents renal remodeling after ischemia/reperfusion injury. Biomedicine & Pharmacotherapy = Biomedecine & Pharmacotherapie 142, 112028. https://doi.org/10.1016/j.biopha.2021.112028.
Jiang, X.S., Liu, T., Xia, Y.F., Gan, H., Ren, W., Du, X.G., 2024. Activation of the Nrf2/ARE signaling pathway ameliorates hyperlipidemia-induced renal tubular epithelial cell injury by inhibiting mtROS-mediated NLRP3 inflammasome activation. Front. Immunol. 15 (April), 1–16. https://doi.org/10.3389/fimmu.2024.1342350.
Joshi, S., Jindal, P., Gautam, S., Singh, C., Patel, P., Gupta, G. Das, Kurmi, B. Das, 2025. Mini review on the lyophilization: a basic requirement for formulation development and stability modifier. Assay Drug Dev. Technol. 23 (4), 180–194. https://doi.org/10.1089/adt.2024.122.
Jumepaeng, T., Pongpun, N., 2020. Development of sample preparation method for organochlorine pesticides analysis in soil samples. AIMS Environmental Science 7, 380–386. https://doi.org/10.3934/environsci.2020025.
Kany, S., Vollrath, J.T., Relja, B., 2019. Cytokines in inflammatory disease. Int. J. Mol. Sci. 20 (23). https://doi.org/10.3390/ijms20236008.
Kara, Y., Kolayli, S., Alberti, A., 2022. Applicability of phenolic profile analysis method developed with RP-HPLC-PDA to some bee product. Braz. Arch. Biol. Technol. 65. https://doi.org/10.1590/1678-4324-2022210384.
Kaur, R., Sood, A., Lang, D.K., Arora, R., Kumar, N., Diwan, V., Saini, B., 2022. Natural products as sources of multitarget compounds: advances in the development of ferulic acid as multitarget therapeutic. Curr. Top. Med. Chem. 22 (5), 347–365. https://doi.org/10.2174/1568026622666220117105740.
Khan, A., Park, T.J., Ikram, M., Ahmad, S., Ahmad, R., Jo, M.G., Kim, M.O., 2021. Antioxidative and anti-inflammatory effects of Kojic acid in Aβ-Induced mouse model of alzheimer's disease. Mol. Neurobiol. 58 (10), 5127–5140. https://doi.org/10.1007/s12035-021-02460-4.
Kim, S., Chen, J., Cheng, T., Gindulyte, A., He, J., He, S., Li, Q., Shoemaker, B.A., Thiessen, P.A., Yu, B., Zaslavsky, L., Zhang, J., Bolton, E.E., 2023. PubChem 2023 update. Nucleic Acids Res. 51 (D1), D1373–D1380. https://doi.org/10.1093/nar/gkac956.
Kizilirmak, C., Bianchi, M.E., Zambrano, S., 2022. Insights on the NF-κB System using live cell imaging: recent developments and future perspectives. Front. Immunol. 13, 886127. https://doi.org/10.3389/fimmu.2022.886127.
Kunchandy, E., Rao, M.N.A., 1990. Oxygen radical scavenging activity of curcumin. Int. J. Pharm. 58 (3), 237–240. https://doi.org/10.1016/0378-5173(90)90201-E.
Lanez, E., Zegheb, N., Lanez, T., 2023. In silico ADMET, toxicological analysis, molecular docking studies and molecular dynamics simulation of Afzelin with potential antibacterial effects against Staphylococcus aureus. Turkish Computational and Theoretical Chemistry 7, 10–16. https://doi.org/10.33435/tcandtc.1196422.
Lanez, T., Lanez, E., 2016. A molecular docking study of N-Ferrocenylmethylnitroanilines as potential anticancer drugs. International Journal of Pharmacology, Phytochemistry and Ethnomedicine 2, 5–12. https://doi.org/10.18052/www.scipress.com/IJPPE.2.5.
Lanez, T., Lanez, M., Lanez, R., Laanez, E., Talbi-Lanez, B., 2025. Computational screening of novel nitroimidazole candidates: targeting key enzymes of oral anaerobes for anti-parasitic potential. Curr. Drug Discov. Technol. 22 (4), e15701638326365. https://doi.org/10.2174/0115701638326365241029080310.
Laraoui, H., Lanez, E., Zegheb, N., Adaika, A., Lanez, T., Benkhaled, M., 2023. Anti-diabetic activity of flavonol glucosides from Fumana montana pomel: in vitro analysis, in silico docking, ADMET prediction, and molecular dynamics simulations. ChemistrySelect 8. https://doi.org/10.1002/slct.202204512.
Larbi, B.A., Lanez, E., Bekkar, Y., Adaika, A., Lanez, T., Nesba, K., Bechki, L., 2025. Evaluation of FERROCENYLMETHYLNUCLEOBASES derivatives interacting with dna: insights from electrochemical, spectroscopic, dft calculation, molecular docking and molecular dynamic simulations. Stud. Univ. Babes-Bolyai, Chem. 70, 111–132. https://doi.org/10.24193/subbchem.2025.1.08.
Laskowski, R.A., Swindells, M.B., 2011. LigPlot+: multiple ligand-protein interaction diagrams for drug discovery. J. Chem. Inf. Model. 51 (10), 2778–2786. https://doi.org/10.1021/ci200227u.
Lawrence, T., 2009. The nuclear factor NF-kappaB pathway in inflammation. Cold Spring Harbor Perspect. Biol. 1 (6), a001651. https://doi.org/10.1101/cshperspect.a001651.
Lekmine, S., Boussekine, S., Kadi, K., Martín-García, A.I., Kheddouma, A., Nagaz, K., Bensouici, C., 2020. A comparative study on chemical profile and biological activities of aerial parts (stems, flowers, leaves, pods and seeds) of astragalus gombiformis. Biocatal. Agric. Biotechnol. 27, 101668. https://doi.org/10.1016/j.bcab.2020.101668.
Leyva-López, N., Gutierrez-Grijalva, E.P., Ambriz-Perez, D.L., Heredia, J.B., 2016. Flavonoids as cytokine modulators: a possible therapy for inflammation-related diseases. Int. J. Mol. Sci. 17 (6). https://doi.org/10.3390/ijms17060921.
Li, J., Chen, J., Lan, H.-Y., Tang, Y., 2023. Role of C-Reactive protein in kidney diseases. Kidney Dis. 9 (2), 73–81. https://doi.org/10.1159/000528693.
Libby, P., 2007. Inflammatory mechanisms: the molecular basis of inflammation and disease. Nutr. Rev. 65 (12 Pt 2), S140–S146. https://doi.org/10.1111/j.1753-4887.2007.tb00352.x.
Liu, B., Lv, D., 2023. Prognostic value of C-reactive protein to albumin ratio for mortality in acute kidney injury. BMC Nephrol. 24 (1), 44. https://doi.org/10.1186/s12882-023-03090-9.
Lu, Y., Zhu, Y., Feng, S., Cong, Q., Chen, S., Zeng, Y., Song, K., Hu, J., 2025. Caffeic acid phenethyl ester protects renal tubular epithelial cells against ferroptosis in diabetic kidney disease via restoring PINK1-mediated mitophagy. Mol. Med. 31 (1), 264. https://doi.org/10.1186/s10020-025-01318-y.
M, A., I, M.A., Ramalingam, K., S, R., 2023. Evaluation of the anti-inflammatory, antimicrobial, antioxidant, and cytotoxic effects of chitosan thiocolchicoside-lauric acid nanogel. Cureus 15 (9), e46003. https://doi.org/10.7759/cureus.46003.
Ma, Q., Hao, S., Hong, W., Tergaonkar, V., Sethi, G., Tian, Y., Duan, C., 2024. Versatile function of NF-κB in inflammation and cancer. Exp. Hematol. Oncol. 13 (1), 68. https://doi.org/10.1186/s40164-024-00529-z.
Madi, N., Boukerb, A.M., Mekdade, L., Ikhlef, A., Meghezzi, A., Selmania, A., Connil, N., 2025. In vitro and in silico assessment of the probiotic and technological potential of Lacticaseibacillus rhamnosus MW019593 isolated from Algerian cow's milk. Probiotics Antimicrob. Proteins. https://doi.org/10.1007/s12602-025-10508-3.
Mahmoud, A.M., Hussein, O.E., Hozayen, W.G., Bin-Jumah, M., Abd El-Twab, S.M., 2020. Ferulic acid prevents oxidative stress, inflammation, and liver injury via upregulation of Nrf2/HO-1 signaling in methotrexate-induced rats. Environ. Sci. Pollut. Res. Int. 27 (8), 7910–7921. https://doi.org/10.1007/s11356-019-07532-6.
Manimaran, D., Tessema, A., Yadav, M.G., Parthasarathi, S., Palanisamy, V., 2025. Current perspectives in detection of bioactive compounds from Costus spicatus through GC – MS and LC-MS/MS : antioxidant properties and in silico analysis for industrial applications. https://doi.org/10.1155/bri/9599942.
Middleton, E.J., Kandaswami, C., Theoharides, T.C., 2000. The effects of plant flavonoids on mammalian cells: implications for inflammation, heart disease, and cancer. Pharmacol. Rev. 52 (4), 673–751.
Mitra, P., Jana, S., Kandar, K., Roy, S., 2025. Exploring the therapeutic effect of flavonoids on kidney health. Curr. Pharmaceut. Anal. 21. https://doi.org/10.1016/j.cpan.2025.06.001.
Morris, G.M., Huey, R., Lindstrom, W., Sanner, M.F., Belew, R.K., Goodsell, D.S., Olson, A.J., 2009. AutoDock4 and AutoDockTools4: automated docking with selective receptor flexibility. J. Comput. Chem. 30 (16), 2785–2791. https://doi.org/10.1002/jcc.21256.
Mouada, H., Stiti, M.Z., Zafar, I., Boutarfaia, A., Djellaili, L., Berregouba, F.L., Aissani, S., 2025. GC-MS analysis, molecular docking, dynamics and ADMET profiling of Algerian Origanum vulgare essential oil compounds as potential COVID-19 inhibitors. Journal of Computational Biophysics and Chemistry 24 (8), 1009–1022. https://doi.org/10.1142/S2737416525500073.
Mukherjee, P.K., Singha, S., Kar, A., Chanda, J., Banerjee, S., Dasgupta, B., Haldar, P.K., Sharma, N., 2022. Therapeutic importance of cucurbitaceae: a medicinally important family. J. Ethnopharmacol. 282, 114599. https://doi.org/10.1016/j.jep.2021.114599.
Nafees, S., Rashid, S., Ali, N., Hasan, S.K., Sultana, S., 2015. Rutin ameliorates cyclophosphamide induced oxidative stress and inflammation in wistar rats: role of NFκB/MAPK pathway. Chem. Biol. Interact. 231, 98–107. https://doi.org/10.1016/j.cbi.2015.02.021.
Nathan, C., Ding, A., 2010. Nonresolving inflammation. Cell 140 (6), 871–882. https://doi.org/10.1016/j.cell.2010.02.029.
Neamah, G.A.K., Alkhfaji, M.A.S., Shaheed, H.S., 2023. The antioxidant role of pumpkin (Cucurbita pepo) seed extract against acute reproductive toxicity by uranyl acetate in male rats. Journal of Advanced Veterinary and Animal Research 10 (4), 647–653. https://doi.org/10.5455/javar.2023.j720.
Ng, C., Kim, M., Yanti, Kwak, M.-K., 2025. Oxidative stress and NRF2 signaling in kidney injury. Toxicol. Res. 41 (2), 131–147. https://doi.org/10.1007/s43188-024-00272-x.
O'Boyle, N.M., Banck, M., James, C.A., Morley, C., Vandermeersch, T., Hutchison, G.R., 2011. Open Babel: an open chemical toolbox. J. Cheminf. 3, 33. https://doi.org/10.1186/1758-2946-3-33.
Pabla, N., Dong, Z., 2008. Cisplatin nephrotoxicity: mechanisms and renoprotective strategies. Kidney Int. 73 (9), 994–1007. https://api.semanticscholar.org/CorpusID:6313214.
Pires, D.E.V., Blundell, T.L., Ascher, D.B., 2015. pkCSM: predicting small-molecule pharmacokinetic and toxicity properties using graph-based signatures. J. Med. Chem. 58 (9), 4066–4072. https://doi.org/10.1021/acs.jmedchem.5b00104.
Radwan, A.M., Karhib, M., Fatoh, S.A., Massoud, A., Tousson, E., 2023. Curcumin alleviates thioacetamide-induced kidney toxicity in rats: enhancing antioxidant system, and attenuating oxidative stress, DNA damage, and inflammation. Biomedical and Pharmacology Journal 16 (1), 441–450. https://doi.org/10.13005/bpj/2625.
Rahman, M.M., McFadden, G., 2011. Modulation of NF-κB signalling by microbial pathogens. Nat. Rev. Microbiol. 9 (4), 291–306. https://doi.org/10.1038/nrmicro2539.
Rahmani, S., Naraki, K., Roohbakhsh, A., Hayes, A.W., Karimi, G., 2023. The protective effects of rutin on the liver, kidneys, and heart by counteracting organ toxicity caused by synthetic and natural compounds. Food Sci. Nutr. 11 (1), 39–56. https://doi.org/10.1002/fsn3.3041.

Rastogi, S., Iqbal, M., Ohri, D., 2018. In vitro study of anti-inflammatory and antioxidant activity of some medicinal plants and their interrelationship. Asian J. Pharmaceut. Clin. Res. 11, 195. https://doi.org/10.22159/ajpcr.2018.v11i4.23583.

Salehi, B., Sharifi-rad, J., Capanoglu, E., Adrar, N., Catalkaya, G., Shaheen, S., Jaffer, M., Giri, L., Suyal, R., Jugran, A.K., Calina, D., Docea, A.O., Kamiloglu, S., Kregiel, D., Antolak, H., Pawlikowska, E., Sen, S., Acharya, K., Bashiry, M., et al., 2019. Applied sciences cucurbita plants: from farm to industry. Appl. Sci. 9 (3387), 1–21. https://www.mdpi.com/2076-3417/9/16/3387.

Srinivasan, M., Sudheer, A.R., Menon, V.P., 2007. Ferulic acid: therapeutic potential through its antioxidant property. J. Clin. Biochem. Nutr. 40 (2), 92–100. https://doi.org/10.3164/jcbn.40.92.

Suhendra, M., Juliandi, B., Darusman, H.S., Sadiah, S., Fitmawati, Budiarti, S., Rianti, P., 2025. Phytochemical analysis and antioxidant activity from Phanera semibifida stem and leaves extracts using LC-MS/MS. Biodiversitas 26 (1), 500–508. https://doi.org/10.13057/biodiv/d260149.

Wang, Y.-N., Wu, X., Shan, Q.-Y., Yang, Q., Yu, X.-Y., Yang, J.-H., Miao, H., Cao, G., Zhao, Y.-Y., 2025. Acteoside-containing caffeic acid is bioactive functional group of antifibrotic effect by suppressing inflammation via inhibiting AHR nuclear translocation in chronic kidney disease. Acta Pharmacol. Sin. 46 (11), 2975–2988. https://doi.org/10.1038/s41401-025-01598-4.

Wang, Y., You, Y.-K., Guo, J., Wang, J., Shao, B., Li, H., Meng, X., Lan, H.-Y., Chen, H., 2025. C-reactive protein promotes diabetic kidney disease via Smad3-mediated NLRP3 inflammasome activation. Mol. Ther. : The Journal of the American Society of Gene Therapy 33 (1), 263–278. https://doi.org/10.1016/j.ymthe.2024.11.018.

Weremczuk-Jeżyna, I., Gonciarz, W., Grzegorczyk-Karolak, I., 2023. Antioxidant and anti-inflammatory activities of phenolic acid-rich extract from hairy roots of Dracocephalum moldavica. Molecules 28 (19). https://doi.org/10.3390/molecules28196759.